Continued Development of Earthquake Load and Resistance Factor Design Guidelines

Report 1

Concrete Gravity Base Structures LRFD Guidelines

by

Professor Robert Bea

Marine Technology & Management Group

Department of Civil & Environmental Engineering

University of California at Berkeley

March 1998

this page left blank intentionally

Table of Contents

this page left blank intentionally

Chapter 1

Introduction

1.0 Objective

The objective of this study is to continue development of earthquake load and resistance factor design (LRFD) guidelines as follows:

1) concrete gravity based structure (GBS) LRFD guidelines, and

2) seismic hazard characterizations.

This report summarizes the results of the first part of this study; concrete GBS LRFD guidelines.

1.1 Background

A first-generation LRFD ISO guideline for design of steel, pile supported, template-type platforms to resist earthquake induced loading has been developed. This guideline was based on the API RP 2A LRFD guideline and on the collective experience and judgment of the ISO P5 committee members. During the first generation developments, limited verification studies of the entire process were performed, there was limited documentation of the background for some of the key developments, and there were additional topics that needed to be addressed. These topics have been discussed and the P5 committee recommended that additional studies be conducted on the two topics cited above.

The basic format for an earthquake design guideline for concrete GBS has been developed by the P5 committee This guideline is included as Appendix A (Karthigeyan, 1995). A number of additional topics need to be developed before the ISO earthquake guidelines for concrete GBS can be completed. The first is to address the unique characteristics of concrete, gravity based platforms subjected to earthquakes. This includes both unique seismic loading considerations and soil-structure interaction modeling, ground motion spatial variability, hydrodynamic mass and damping, effective loading factors that reflect the unique nonlinear performance characteristics of concrete structures, and seismic performance considerations including concrete elements ductility, capacity biases, and uncertainties.

This study was organized as follows:

- obtain background on unique concrete GBS considerations and results from seismic performance analyses and studies.

- develop and detail GBS concrete element biases and uncertainties.

- develop and detail GBS mat foundation biases and uncertainties.

- detail seismic loading effects for the nonlinear of concrete platforms

- develop LRFD factors for GBS loading and concrete element capacities.

- document the GBS LRFD guidelines in a project technical report.

1.2 Unique Aspects

A concrete GBS (Figs. 1.1 and 1.2) can be divided into three primary components: 1) the deck section, 2) the supporting columns, and 3) the gravity base.

Because of the large spans and cantilevers, asymmetric geometry and loadings, and heavy gravity and live loadings, the deck section can experience large earthquake induced vertical and horizontal dynamic loadings.

The supporting columns are parallel cantilever beam columns that receive their support and fixity from the gravity base. These beam columns can be subjected to large static and dynamic axial loadings and large lateral dynamic lateral loadings induced by earthquakes. Because of their large volumes, hydrodynamic mass effects in the supporting columns can be very important. Interactions of the wells and risers inside the supporting columns (Fig. 1.3) can also produce some important effects.

The gravity base is a very large and rigid mat comprised of concrete elements (Fig. 1.1). The gravity base is supported by the sea floor soils that must sustain the vertical and horizontal loadings transmitted to them by the gravity base. Because of its large volume, hydrodynamic mass effects in the gravity base can be very important. Since the earthquake ground motions (free-field) are transmitted to the GBS through the gravity base and the nearby soils (near-field), soil structure interactions (SSI) can also be very important to the dynamic loadings induced in the superstructure. These interactions can have dramatic effects on the stiffness and damping of the GBS system. Because of the wells and risers that must pass through the gravity base (Fig. 2), these elements can impose important limitations on the movements that can be tolerated by the GBS.

Because of its materials and configuration compared with conventional steel, pile supported template-type platforms, a concrete GBS has the following unique and important earthquake design and performance characteristics that were considered during this study:

a. vertical ground motions to performance of deck supporting structure,

b. vertical ground motions at and near the sea floor,

c. variable ground motions over the large dimensions of the base mat,

d. hydrodynamic mass and mass distribution effects in the supporting columns and gravity base,

e. soil - GBS interactions during earthquake ground motions,

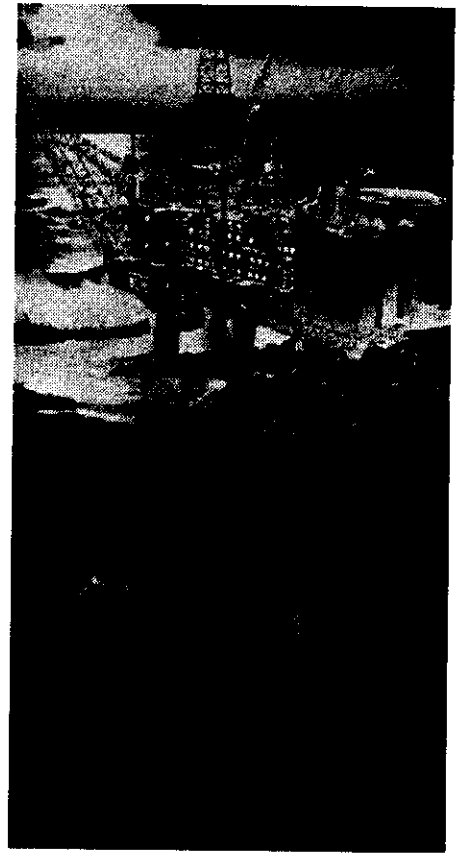f. concrete column ultimate limit state performance characteristics in earthquake loadings.
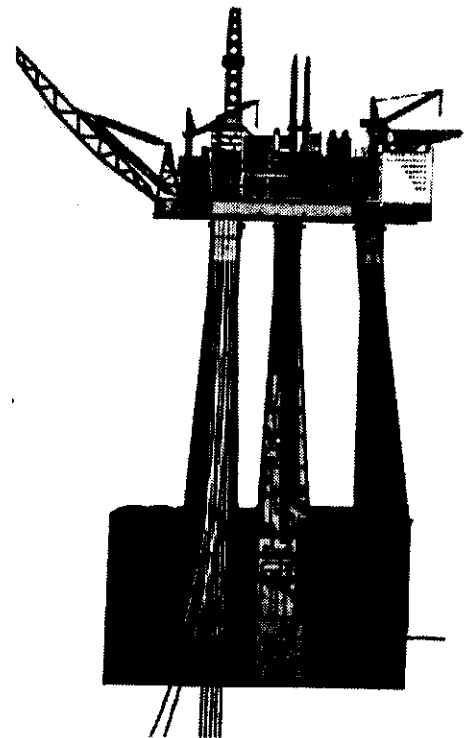

Fig. 1.1 - Gullfaks C GBS

Fig. 2 - GBS section
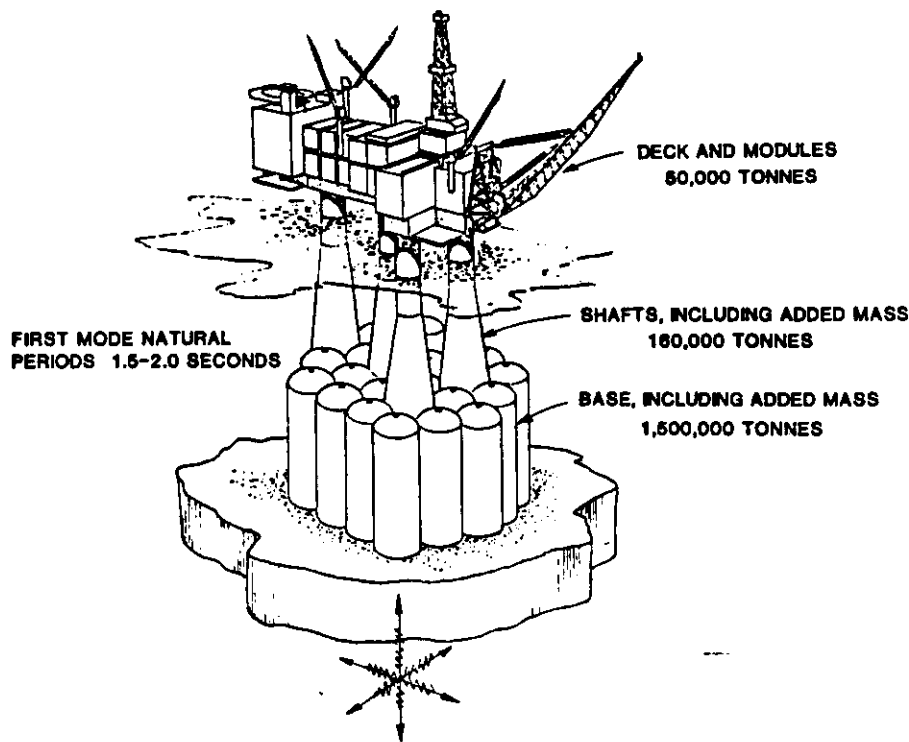
2

FIRST MODE NATURAL
PERIODS 1.5-2.0 SECONDS

DECK AND MODULES
50,000 TONNES

SHAFTS, INCLUDING ADDED MASS
160,000 TONNES

BASE, INCLUDING ADDED MASS
1,500,000 TONNES

Fig. 1.3 - Unique Aspects of Concrete GBS

1.3 Earthquake LRFD Approach

The earthquake LRFD approach can be expressed analytically as follows (Appendix B):

$$\phi_E \ R_E \geq \gamma_{D1} \ D_1 + \gamma_{D2} \ D_2 + \gamma_{L1} \ L_1 + \gamma_E \ E \dots\dots\dots\dots\dots\dots\dots\dots\dots\dots\dots\dots\dots\dots\dots\dots\dots\dots(1.1)$$

where ϕ_E is the resistance factor for earthquake loadings, R_E is the design capacity of the platform element (e.g. brace, joint, pile) for earthquake loadings as defined by the API RP 2A - LRFD guidelines, γ_{D1} is the self-weight of the structure (dead) loading factor, D_1 is the design dead loading, γ_{D2} is the imposed equipment and other objects loading factor, D_2 is the design equipment loading, γ_{L1} is the consumables, supplies, and vessel fluids (live) loading factor, L_1 is the live loading, γ_E is the earthquake loading factor, and E is the earthquake loading effect developed in the structure or foundation element. This development addresses the definition of the resistance factors, ϕ_E , and the loading factors, γ_E , for loadings induced by earthquakes (Bea, 1997). The dead, equipment and live loading factors are set as $\gamma_{D1} = \gamma_{D2} = \gamma_{L1} = 1.1$.

The earthquake loading factor is determined using a Lognormal format:

$$\gamma_E = Fe \ B_E \ exp \ (0.8 \ \beta_E \ \sigma_E - 2.57 \ \sigma_E) \dots\dots\dots\dots\dots\dots\dots\dots\dots\dots\dots\dots\dots\dots\dots\dots\dots\dots(1.2)$$

where Fe is the median effective loading factor, Be is the median bias (actual / nominal) in the computed earthquake loadings, β_E is the annual Safety Index designated for the platform SSL, σ_E is the total uncertainty associated with the earthquake loadings (standard deviation of the annual maximum earthquake loading), 0.8 is the splitting factor used to separate linearly the uncertainties in earthquake

3

loadings and platform capacities, and the 2.57 is a consequence of defining the elastic design earthquake (Strength Level Earthquake) at an average return period of 200-years (2.57 Standard Normal deviations from the mean).

The effective loading factor for the platform system is expressed as:

$$Fe = [\ \mu\ \alpha\ ]^{-1} \quad\quad\quad\quad\quad\quad\quad\quad\quad\quad\quad\quad\quad\quad\quad\quad\quad\quad\quad\quad\quad\quad\quad (1.3)$$

where μ is the platform system ductility and α is the platform residual strength ratio:

$$\mu = \Delta p\ /\ \Delta e \quad\quad\quad\quad\quad\quad\quad\quad\quad\quad\quad\quad\quad\quad\quad\quad\quad\quad\quad\quad\quad\quad\quad (1.4)$$

$$\alpha = A/\ Aep \quad\quad\quad\quad\quad\quad\quad\quad\quad\quad\quad\quad\quad\quad\quad\quad\quad\quad\quad\quad\quad\quad\quad (1.5)$$

Δp is the maximum plastic displacement that can be developed by the platform system at 'failure', Δe is the displacement at which first significant nonlinear behavior is indicated by the platform system, A is the area under the platform loading - displacement to failure diagram, and Aep is the area under an equivalent elasto-plastic platform loading - displacement to failure diagram.

The total uncertainty associated with the earthquake loadings (σ_E) is expressed as:

$$\sigma_E{}^2 = \sigma_{SE}{}^2 + \sigma_{GS}{}^2 + \sigma_{RS}{}^2 \quad\quad\quad\quad\quad\quad\quad\quad\quad\quad\quad\quad\quad\quad\quad\quad (1.6)$$

where σ_{SE} is the uncertainty in the earthquake horizontal peak ground accelerations, σ_{GS} is the uncertainty related to the local geology and soil conditions and their effects on the ordinates of the earthquake response spectra, and σ_{RS} is the uncertainty associated with the response spectrum method used to determine forces in the elements that comprise the platform.

In development of the proposed ISO earthquake guidelines, Type I (natural, inherent, aleatory) uncertainties are included in σ. The effects of Type II (model, parameter, state, epistemic) uncertainties are introduced with the Biases in loading effects and capacities. This is done to develop as close as possible a correlation with the way in which the target Safety Indices and probabilities of failure were determined.

The platform element resistance factor is determined from:

$$\phi_E = \mathbf{B_{RE}}\ exp\ (-0.8\ \beta_E\ \sigma_{RE}\ ) \quad\quad\quad\quad\quad\quad\quad\quad\quad\quad\quad\quad\quad\quad\quad\quad (1.7)$$

where $\mathbf{B_{RE}}$ is the median bias (actual value / nominal or code value) in the element earthquake loading capacity, and is the σ_{RE} uncertainty in the earthquake loading capacity of the element .

The proposed ISO earthquake LRFD approach proceeds through the following nine steps (Appendix B):

1. Define the structure safety and serviceability level (SSL)

2. Define the earthquake hazard zone (EHZ) and seismotectonic conditions

3. Determine if site specific seismic exposure study is required

4. Define the shape of the normalized mean elastic principal horizontal acceleration response spectrum for a specified damping ratio, soil profile, and seismotectonic condition

5. Determine the uncertainties associated with the seismic exposure, response spectrum, and the methods used to analyze earthquake forces induced in the structure

6. Determine the earthquake loading factor (γ_E) for the elastic response spectra forces

7. Evaluate the biases and uncertainties in the platform element design capacities

8. Determine if a ductility analysis is required and the performance characteristics for the analyses

9. Determine the platform element resistance factors (ϕ_E) for the design code based capacities

The remainder of this report will summarize the study of applications of the foregoing LRFD approach to the unique considerations associated with concrete GBS as outlined in Section 1.2.

In the context of the loading and resistance factor formulation summarized in Eqn. (1) through (7), the key issues included in this study were:

- σ_{RS} - the uncertainty associated with application of the elastic response spectrum method to GBS

- B_E - the bias associated with application of the elastic response spectrum method to GBS

- **Fe** - the effective loading factor associated with the ultimate limit state performance characteristics of concrete GBS

- σ_{RE} - the uncertainty associated with the performance characteristics of GBS elements when subjected to ultimate limit state condition earthquakes, and

- B_{RE} - the bias associated with the analyses of the performance characteristics of GBS when subjected to ultimate limit state condition earthquakes.

These five factors were evaluated to address the potentially unique characteristics of concrete GBS in development of LRFD earthquake design guidelines.

At the outset of these developments it is important to recognize that the single largest source of uncertainty in earthquake effects on concrete GBS is founded in the earthquake ground motions themselves. Fig. 1.4 shows elastic response spectra (3 % damped) for horizontal components of 15 records from a single type source of earthquakes at a single location 50 km from the source for Magnitude 6.5 earthquakes. (Heaton, Hartzell, 1988). The variability that is shown is 'natural' or inherent (Type I). Note in the long period range of primary interest the scatter in the maximum pseudo relative velocities (reflecting the earthquake force effects) have a range that exceeds one order of magnitude. Differences in energy release characteristics of the sources and seismic wave travel paths are reflected in this scatter. This uncertainty coupled with the associated uncertainties due to the magnitudes of earthquakes that could be associated with seismic sources, attenuation of the earthquakes from the sources to the sites, and with local site and geology effects are the dominant sources of uncertainties that must be addressed in development of earthquake guidelines for concrete GBS. These sources of uncertainty are not unique to concrete GBS. They are common to all types of offshore structures.
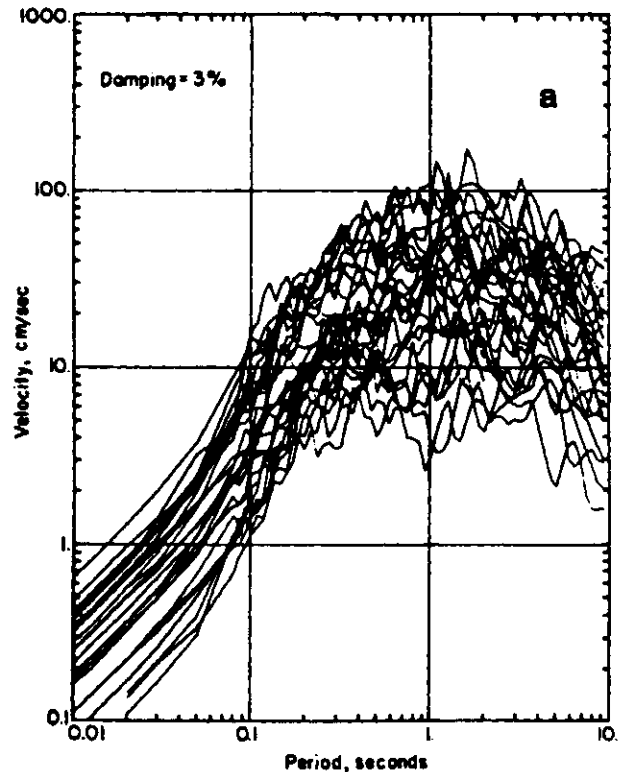

Fig. 1.4 - Response spectra for horizontal components of 15 earthquake records (distance = 50 km, Magnitude = 6.5)

5

this page left blank intentionally

Ground Motion Considerations

2.0 Introduction

Three ground motion considerations important to the performance and response of concrete GBS to earthquakes were considered during this study:

1. The response spectra ordinates in the high frequency range,

2. The ratio of vertical to horizontal response spectra ordinates, and

3. The sea floor motions as affected by the water column.

The results of the study of these three aspects will be summarized in the remainder of this Chapter.

2.1 Response spectra ordinates

Recent studies of response spectra ordinates in the low period range (0.1 sec to 0.3 sec) have indicated that one should expect that these ordinates will vary as a function of both the local soil conditions (soil column classification)and intensity of earthquake motions (Martin, Dobry, 1994; Crouse, McGuire, 1996). Figure 2.1 summarizes the results from the study by Crouse and McGuire of the median amplification factors (Fa = peak horizontal ground acceleration at surface / peak horizontal ground acceleration on rock = PGAs / PGAr) for periods (T) in the range of T = 0.1 sec to 0.3 sec.
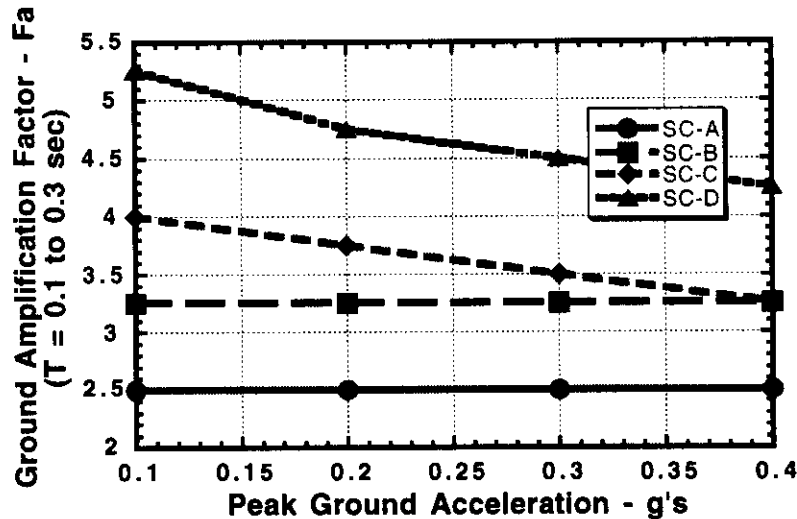

Fig. 2.1 - Amplification factors as function of acceleration level and soil conditions

The site soil conditions indicated as SC-A, B, C, and D correspond to those in the proposed ISO guidelines (Appendix B, Table 3). The amplification factor in this period range presently incorporated into the proposed ISO guidelines is Fa = 2.5 for all soil conditions. These results indicate substantially

larger amplifications in the short period range. While these findings would relatively unimportant for the lateral motions of GBS (T = 2 to 3 sec), the effects would be potentially important for the vertical motions (T = 0.1 to 0.3 sec).

The National Center for Earthquake Engineering Research (NCEER) workshop defined a comparable range of amplification factors for this period range (Martin, Dobry, 1994).

As a result of these findings, the following modifications to the proposed ISO earthquake guidelines are proposed. The elastic design response spectra (Figure 2.2) would be a function of the following variables:

- T = period of system

- D = damping of system

- v = site classification factor for short period range (new factor)

- ψ = site classification factor for long period range
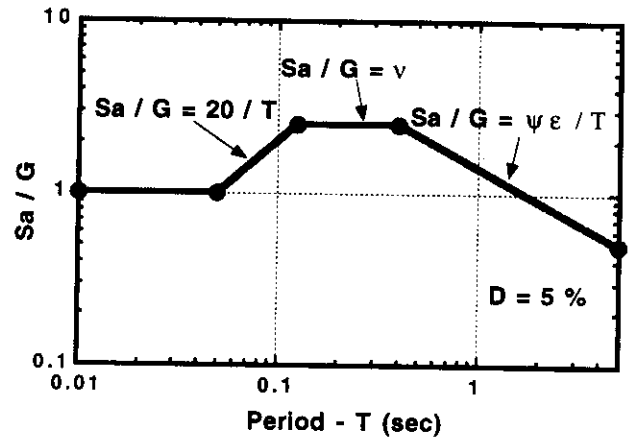
- ε = seismotectonic conditions

Table 2.1 summarizes the elastic design response spectra characteristics based on the results of the work by Crouse and McGuire (1996) and the previous work incorporated into the proposed ISO design response spectra.

Fig. 2.2 - Proposed elastic design response spectra

Table 2.1 - Local geology and soil conditions parameters for design response spectra

Soil Conditions			Seismotectonic Conditions	
Site Class	v	ψ		ε
SC-A	2.5	1.0	Type A	1.0
SC-B	3.3	1.2	Type B	0.8
SC-C	3.5	1.4	Type C	0.9
SC-D	4.5	2.0	Type D	0.8
SC-E	Site specific studies required		Default value	1.0

2.2 Horizontal to Vertical Response Spectra Ordinates

Several recent large magnitude earthquakes have indicated that vertical ground motions can be equal to or greater than the horizontal ground motions. This observation has been particularly true for ground motions close to the epicenter of large magnitude earthquakes. The present ISO guidelines prescribe an elastic design response spectrum for vertical motions that is one-half of the horizontal motions.

Figure 2.2 summarizes results from a recent study of the ratios of vertical to horizontal spectral ordinates as a function of the response frequency (Bozorgnia, Niazi, Campbell, 1995). Results for the Loma Prieta and Taiwan earthquakes are shown. The ratios indicated are mean values. The horizontal line indicated at the ratio of 2/3 references the present Uniform Building Code (UBC) specifications. For near-by earthquakes (R = 10 km), the ratio of the vertical to horizontal spectra ordinate for periods

in the range of T = 0.1 sec are in the range of 1.4 to 1.7. The ratio is close to unity at distances of R = 20 km to 30 km. Comparable results have been found for other large magnitude earthquakes in other semismotectonic zones.

For periods in the range of T = 2 to 3 sec, the ratios are in the range of 0.2 to 0.3 for all distances. Current studies of recordings from different earthquakes generated by different types of seismotectonic environments indicates that these trends are "very likely to be universal." (Bozorgnia, Niazi, Campbell, 1995).

These results show the problems that are associated with specifying a constant ratio of vertical to horizontal spectra ordinates for all periods and distances. The results indicate that the horizontal and vertical spectra have decidedly different shapes.

The author's application of these results to the 'unmodified'[1] ISO response spectra is illustrated in Figure 2.4. The present proposed ISO horizontal and vertical response spectra for Site Classification C (firm alluvium, $v = 3.5$, $\psi = 1.4$) and Type A seismotectonic conditions (shallow crustal faulting, $\varepsilon = 1$). For periods greater than about 0.3 sec, the unmodified vertical response spectra have ordinates that are less than the present proposed ISO guideline vertical spectra. For periods less than 0.3 sec, the unmodified ordinates are substantially larger.

2.3 Vertical Response Spectra Ordinates Modified for Water Column Effects

The foregoing results have been developed based on earthquake ground motion measurements that have been made on land. Measurements of ground motions offshore have indicated that the presence of the water column can have a marked influence on the sea floor motions (Smith, 1997; Sleefe, 1990). The measurements indicate that the vertical motions at the sea floor are much less than would expected based on on-land
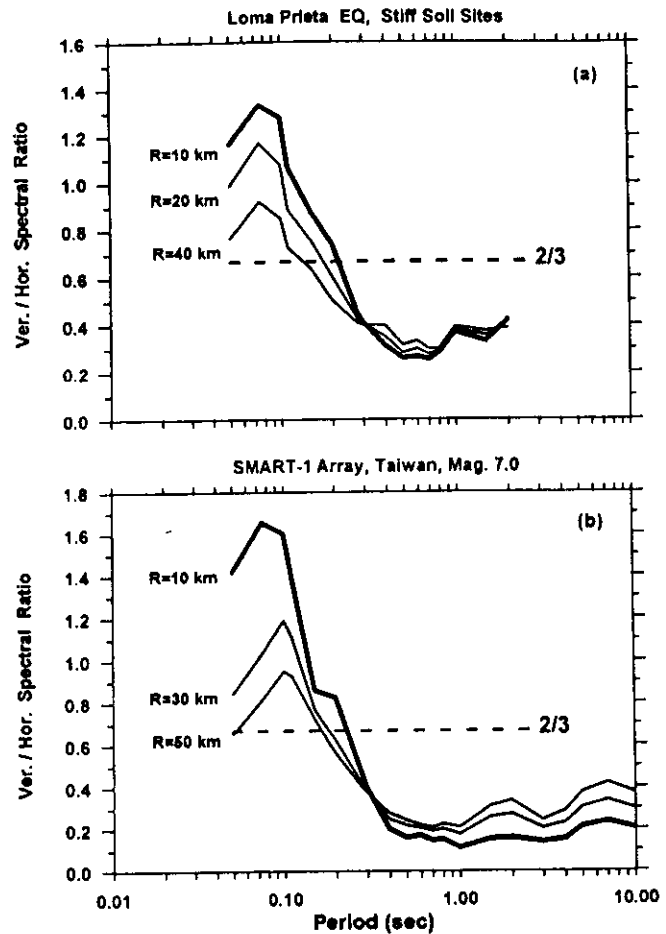

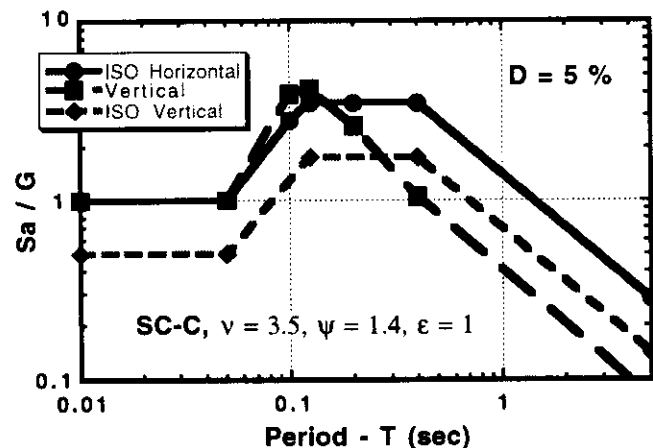Fig. 2.3 - Ratio of Vertical to Horizontal Elastic Response Spectra Ordinates

Fig. 2.4 - Horizontal and Vertical Elastic Response Spectra for SC-C, $\varepsilon = 1.0$

---

[1] unmodified for water column effects

9

measurements. For mat supported structures that receive the majority of their input motions from soils that are located near the sea floor, this can be an important consideration.

For vertically incident earthquake compression waves, the ratio of the reflected to the incident wave amplitude at the ground surface is a function of the impedance ratio, IR, at the ground surface:

$$IR = \rho s \, Vs \, / \, \rho a \, Va \dots\dots\dots (2.1)$$

where ρ is the mass density of the soil (s) and air (a), and V is the compression wave velocity in the two media. On land, this impedance ratio is very large, and one would expect almost total reflection of the energy at the ground surface. This would indicate a doubling of the amplitude of the incident compression waves at the ground - air interface.

In water, the compression wave velocity in the water and in the water saturated sediments would be almost the same. The density difference would be a factor of about 2. This would indicate that about 50 % of the compression wave would be transmitted through the interface and the remaining 50 % would be reflected. The total wave amplitude at the interface would be 1.5 times the incident amplitude or 75 % of the amplitude expected at an air - soil interface.

This analysis assumes that the water is infinitely deep and ignores the reflection of the incident compression waves at the water - air interface. Crouse and Quilter (1991) developed an analysis that includes the finite water column effects. Depending on the water depth, some frequencies can be reinforced and amplified by the finite water depth, while others can be canceled. The analyses performed by Crouse indicates that the peak vertical accelerations at the sea floor can be reduced by as much as 50 % (Crouse, Quilter, 1991; Dolan, Crouse, Quilter, 1992). These observations are in agreement with the analyses of recorded earthquakes at the sea floor reported by Smith (1997) and Sleefe (1990)

The earthquake ground motions in the vicinity of the sea floor are the result of a very complex variety of wave forms, frequencies, and incidence angles. Thus, the foregoing simplified analyses can be relied upon only to provide some insights into the potential effects of the water column on the vertical movements at the sea floor. Measurements of earthquake movements at the sea floor provide the only reliable source of information to quantify these effects. The measurements that are available confirm the inferences that have been drawn based on simplified analyses.

Figure 2.5 summarizes the results for the water column modified vertical response spectra compared with the present ISO vertical response spectra. The present ISO vertical response spectra provides a conservative envelope to the modified vertical spectra for periods greater than about 0.2 sec. However, the present ISO vertical response spectrum is somewhat unconservative for periods less than about 0.2 sec.

Until better information becomes available, it is the author's conclusion that the present proposed ISO guidelines for vertical response spectra provide a reasonable, and likely somewhat conservative approximation to the vertical movements that can be expected at the bases of GBS.
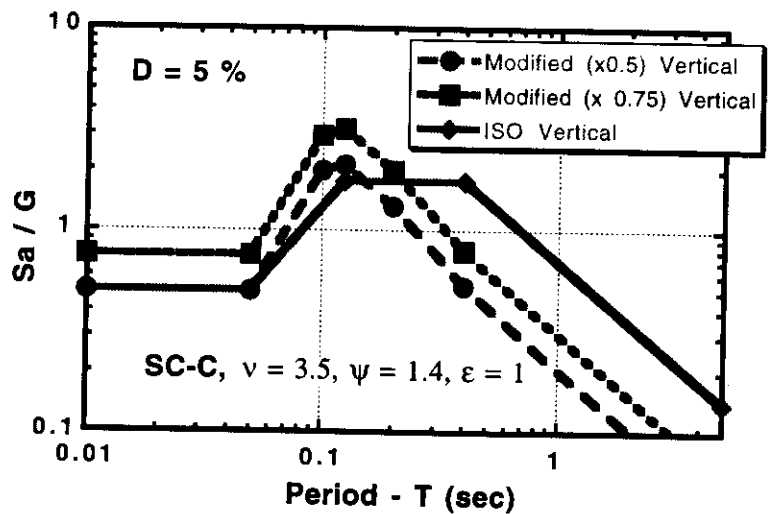

Fig. 2.5 - Water Column Modified Vertical Response Spectra

<div align="right">

Chapter 3

</div>

Design Loading Analysis Considerations

3.0 Introduction

The following earthquake design loading analysis considerations were reviewed during this study:

1. Spatial variability in the earthquake ground motions,

2. Response spectra based analytical methods,

3. Hydrodynamic considerations, and

4. Measured and predicted responses of GBS in earthquakes.

The results of the study of these three aspects will be summarized in the remainder of this Chapter.

3.1 Spatial Variability

Analyses of GBS subjected to earthquakes are based on the same earthquake ground motion input to all parts of the GBS foundation (Fig. 3.1). For structures whose geometry is small compared with the wave lengths that comprise the intense earthquake ground motions, this is reasonable. However, for structures whose geometry could be in the same range as the earthquake ground motion wave lengths, there could be important spatial considerations (Newmark, 1969; Scanlan, 1976).

Fig. 3.2 summarizes results of the study of earthquake horizontal wave propagation on the motions of structures by Scanlan(1976). The wave number (R_n) in Fig. 3.2 is:

$$R_n = 2 \pi L / \lambda_n \dots\dots\dots(3.1)$$

L is the width of the foundation in the direction of wave propagation and λ_n is the earthquake motion wave length:

$$\lambda_n = c_n T_n \dots\dots (3.2)$$

c_n is the wave speed (celerity) and T_n is the wave period.

The diameter of GBS foundations are in the range of 150 m to 200 m. The shear wave velocities of the sea floor soils that support the GBS can be in this same range. Given that GBS response periods were in the range of 2 sec to 3 sec, one would expect that there could be important spatial effects on the earthquake ground motions that are actually transmitted to the base of a GBS.
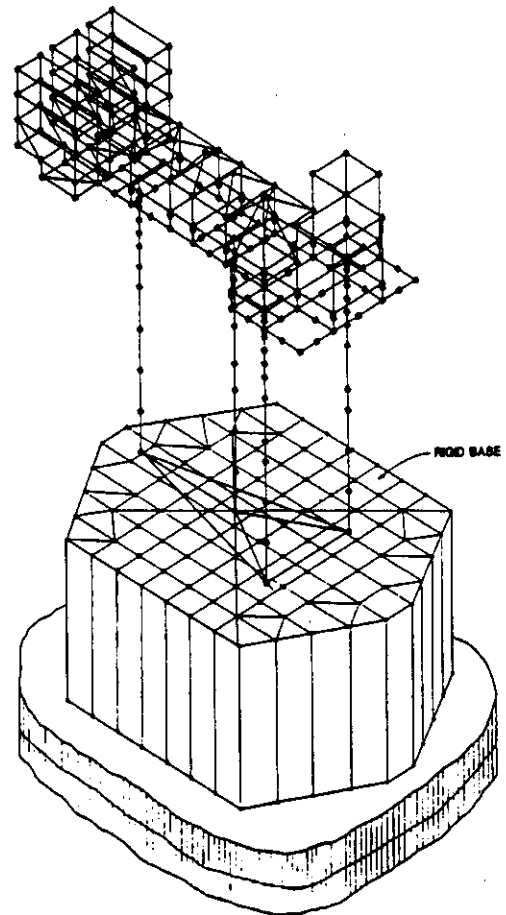
Fig. 3.1 - Analytical Model for GBS Response Spectra Evaluation

Wave amplitude reductions vs wave number
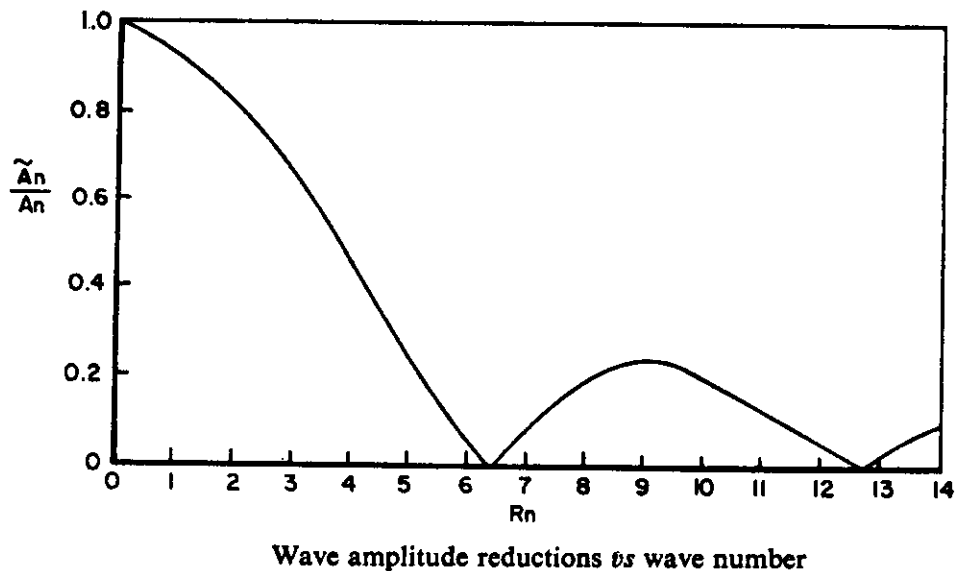
Fig. 3.2 - **Wave amplitude reduction factor (ordinate) versus structure width - wave length ratio**

For example, for a 150 m wide GBS foundation sited in sediments that had a shear wave velocity of 200 m/s, and for a ground motion period of 2 sec, sinusoidal earthquake ground motions would have a length of 400 m. $R_n = 2.4$, and the amplitude ratio $A_{en} / A_n \approx 0.8$; the 'effective' ground motion amplitude for the foundation would be 80 % of the free field ground motion amplitude. For a soil shear wave velocity of 100 m/s (soft cohesive soils), $A_{en} / A_n \approx 0.3$.

The earliest studies of earthquake spatial effects were conducted by Newark (1969) and Yamahara (1970). Their work indicated that there would be reduction of the translation motion of a large rigid foundation with decreasing period of the ground motion down to a period which is about 75 % of the natural period of the soil column. The reduction remains almost constant for lower periods with an average value which is about 50 % of the amplitude at the soil surface (free field). For relatively flexible structures on stiff soils, the reduction in the motion at the frequency of primary interest (fundamental period of the soil-structure system) would be small. However, for relatively stiff structures on flexible soils, the reduction in the motion at the frequency of primary interest can be significant. The reduction in the horizontal motions is accompanied by a rocking component. The average amplitude of the vertical motion at the edge of the foundation due to this rotation is about 30 % of the amplitude of the horizontal motion at the free surface.

Extensive studies of foundation motions due to trains of earthquake body and surface waves at different angles have been conducted (Scalan, 1976; Luco, 1980; Pais, Kausel, 1985; Der Kiureghian, 1996). Several important effects have been identified including incoherence (ground motions different at different points at same time), wave passage (coherent but different at different points), attenuation (decreasing amplitude of components during passage), and site response (scattering due to soil layering). Theoretical models have been developed to characterize each of these effects (Der Kiureghian, 1996). However, sufficient measured data are not available to provide all of the information required for the theoretical models (Aki, 1988). Some data is available for specific settings and earthquake conditions. (Schneider, et al, 1992; Somerville, et al., 1988; Zerva, Harada, 1994; Harichandran, 1988). These models are all highly site and sources specific. At this time, no generalizations appropriate for a design guideline are available. As appropriate, these effects can be incorporated in site specific studies.

It is important to recognize that the models all indicate that a reduction in the lateral motions can be expected for very large rigid foundations embedded in flexible soils. However, these reduced lateral motions will be accompanied by significant rocking and torsional motions.

12

In similar large geometry and rigid base structures (e.g. nuclear power plants, dams), explicit recognition of these spatial motion effects presently are omitted in the design analytical models (Brookhaven National Laboratory, 1994; Working Group on Quantification of Uncertainties, 1986). It is likely that a significant spatial effect can be present under some conditions (e.g. very soft soil locations whose earthquake ground motions are dominated by surface waves). It is the author's conclusion that current technology is not sufficiently developed to allow explicit introduction of the spatial effects into design of concrete GBS platforms.

3.2 Response Spectra Analyses

The analytical approach incorporated into the proposed ISO guidelines is an elastic response spectra based approach that is used to determine the design loadings, forces, and stresses in the elements and components that comprise the GBS. The issue that was considered during this study regarded the bias that could be introduced through the application of such an approach when compared with other potentially more accurate approaches such as time-history analyses.

The results from response spectra and time history analyses depend greatly on how SSI effects are modeled (Kausel, Sunder, 1982; Veletsos, 1977; Watt, 1978; Watt, et al, 1978; Whittacker, 1987; Penzien, Tseng, 1976). Response spectra methods generally incorporate frequency independent discrete elements (springs, dashpots) that are intended to simulate the SSI behavior (Fig. 3.3). The first step in these analyses is to define input motions that are appropriate for the analysis of the SSI behavior. For the proposed ISO guidelines, these input motions are incorporated into the three component response spectra that are intended to be applied at the sea floor (free field motions).

The second step is to use a three-dimensional, nonlinear, soil-foundation analytical model to derive frequency independent linear springs and dashpots (Fig. 3.4) (PMB Systems Engineering Inc., 1984). These springs and dashpots are then used to support the detailed model of the GBS superstructure above the relatively rigid foundation base (Fig. 3.2). Nonlinear behavior in the foundation soils must be

Fig. 3.3 - Response Spectra SSI Simulation

Fig. 3.4 - GBS Base Mat - Soil Interaction Model

evaluated using 'equivalent linear' approximations to the nonlinear SSI (Penzien, Tseng, 1976; Watt, 1978). Generally, the analyses must be performed recursively so that a reasonable approximation to the nonlinear SSI is developed for the Strength Level Earthquake (SLE, design level) conditions.
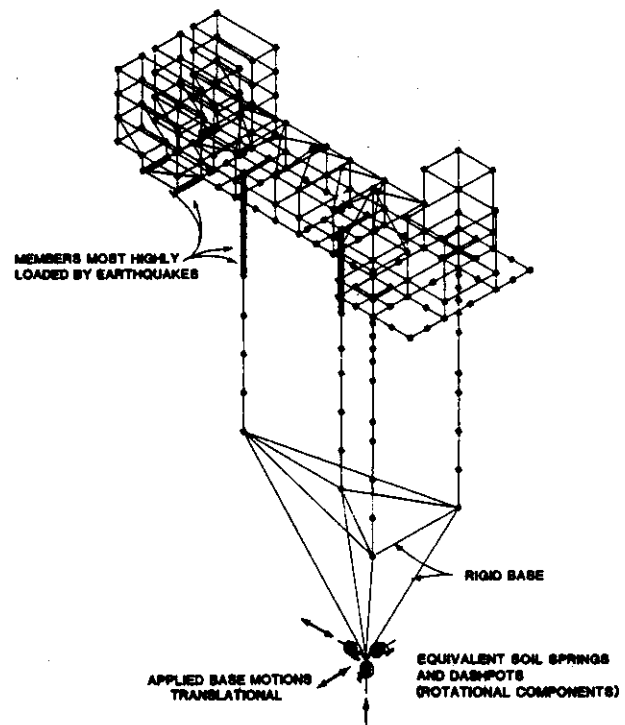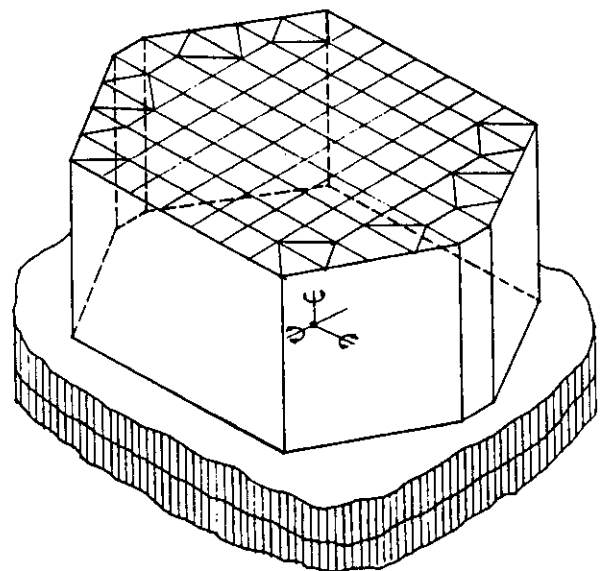
Reasonable equivalent linear discrete elements (springs) or more complex frequency dependent impedance functions (Kausel, Sunder, 1982) can be developed to simulate the foundation translational and rotational stiffness (Fig. 3.4).

While this approach is relatively straight forward for development of the linear springs to simulate the stiffness of the foundation and soils, it is less straight forward for development of the damping that should be utilized in the response spectra analyses. Uniform modal damping must be used in the response spectra analyses. The foundation damping is potentially very different in magnitude than that in the superstructure (mat, legs, hydrodynamic).

The foundation damping is derived from two fundamental sources:

1) hysteretic damping due to the nonlinear behavior of the soils, and

2) radiation damping due to radiation of energy away from the GBS base mat.

Neither of these two sources of damping are simple to determine (Bea, 1984; Veletsos, 1977; Kausel, Sunder, 1982; Watt, et al, 1978; Wolf, 1985).

The hysteretic damping is a function of the strains induced in the foundation soils by the movements of the GBS foundation. The radiation damping is a function of the geometry, mass, and stiffness of the GBS foundation, frequency of movements, the nonlinear behavior of the soils, and the layering in the soils (potentially reflecting energy back to the foundation). At low levels of strains in the soils for which hysteretic damping is small (GBS on relatively stiff soils), the radiation damping will be the dominant component of damping. At high levels of strains in the soils for which hysteretic damping is large (GBS on relatively flexible soils), the radiation damping will be relatively small. Layering in the soils in which the impedance ratios between the layers are very large, will tend to dramatically reduce the radiation damping. No simple method to define the foundation damping has been developed to simulate these complex interactions and effects (Yokel, Bea, 1986).

Given that modern finite element methods are used in which nonlinear soil behavior, soil layering, wave propagation, and energy absorbing boundaries can be simulated, then these effects can be reasonably accurately evaluated to determine the equivalent amount of viscous damping for each of the modes of GBS motion for the primary periods of interest.

The next challenge is that of combining the foundation damping with that associated with the superstructure motions to define an overall effective modal damping for the GBS system. Based on a study of the response of systems to earthquakes Veletsos (1977) proposed the following relationship:

$$D = Df + [Ds / (T' / T)^3] \quad\quad (3.3)$$

where D is the combined effective damping ratio, Df is the foundation damping ratio, Ds is the damping ratio associated with the superstructure movements, T is the fixed base structure period, and T' is the flexible base structure period. Note that the foundation damping is not simply added to the structure.

Fig. 3.5 summarizes experimental data obtained for the damping associated with a heavily reinforced concrete nuclear power plant structures (Farrar, Bennet, 1988). The data indicate that the damping is a function of the intensity of the earthquake excitation or the strains induced in the concrete elements. Damping ratios in the range of 5 % to 10 % are indicated.
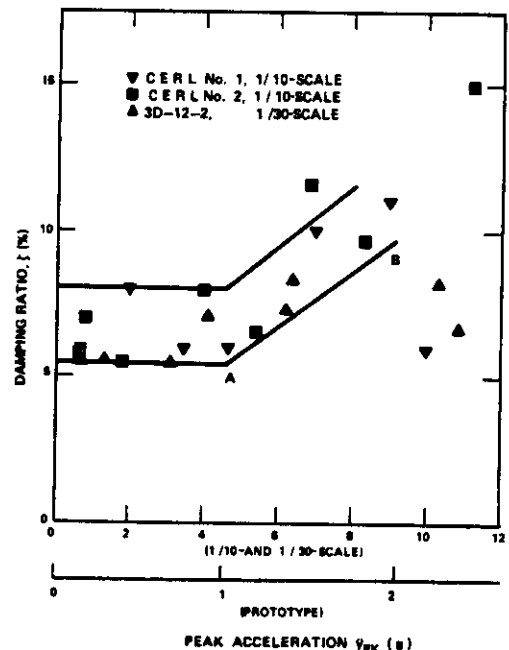

Fig. 3.5 - Measured damping in concrete nuclear power plant structures

14

For example, Df = 10 %, Ds = 5 %, T' / T = 1.5, D = 11.5 %; the foundation is responsible for 87 % of the system damping. Note also that while the damping associated with the concrete superstructure and the hydrodynamic interactions (drag damping and wave making at the surface) could be relatively small, the overall system damping can be relatively large.
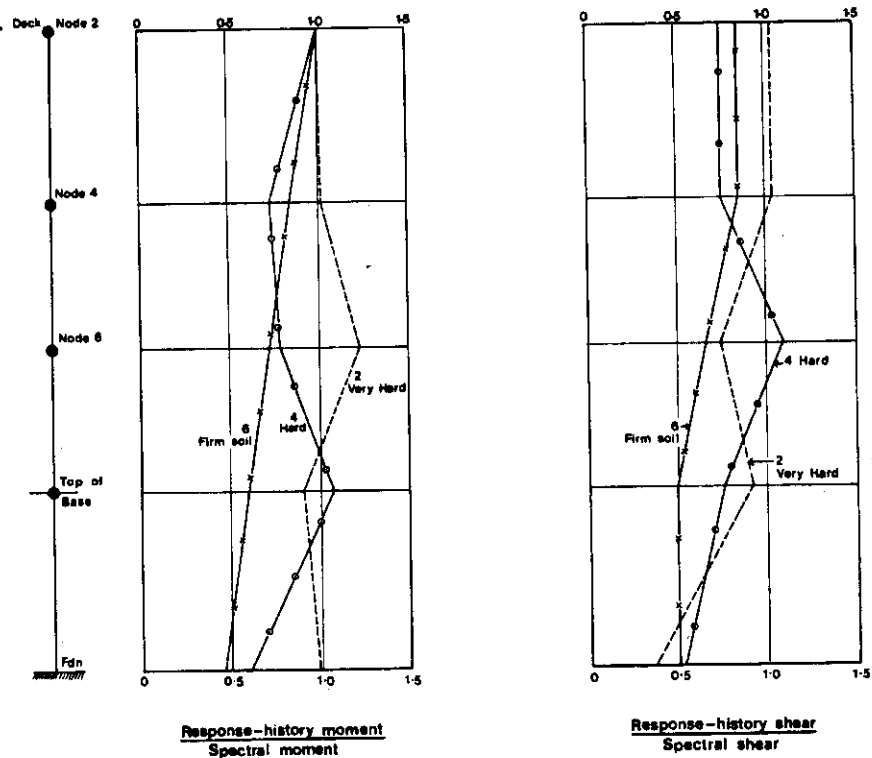
Given a GBS subjected to an SLE, it would be difficult to justify an effective damping ratio for lateral motions less than 10 %. Given D = 10 %, the ordinates on the proposed ISO elastic response spectra would be reduced by a factor of:

K = 0.33 ln (100 % / 11.5 %) =
0.71..................................

If the equivalent system damping were 20 %, then the reduction factor would be K = 0.51. Such system damping would be reasonable for a concrete GBS. The response spectra based forces are influenced significantly by the damping that is utilized in deriving the SLE forces.

Another analytical consideration reviewed during this study was the method used to combine modes in the response spectra. The basis for this review were results published by Watt, et al (1978) on their studies of GBS responses to earthquakes. A summary of their results is given in Fig. 3.6 for a range of foundation stiffness and damping conditions (firm to very hard). The SRSS (square root of sum of squares) method

Fig. 3.6 - Comparison of Results from Response Spectra and Time History Analyses of GBS

was used to combine the response spectra modes. Mean results are indicated for the time history analyses. The results indicate that the SRSS based response spectra analyses generally results in a conservative estimate of the shears and overturning moments in the GBS, particularly at the base of the GBS. The bias (true = time history / nominal = SRSS response spectra) is about 0.5 for the shears at the base of the GBS and closer to unity higher in the structure. Overturning moments biases tend to be closer to unity.

The foregoing results indicate that depending on details of the response spectrum based design analyses, focused in the foundation analytical models and parameters that chiefly determine system damping, and in details of the response spectrum method (elastic, modal combinations), there could be significant biases in the loadings determined from the design analyses. Median biases in the range of B_E = 1.0 to 0.5 could be present (Working Group on Quantification of Uncertainties, 1986). The natural variability associated with the computed earthquake design forces (given free field soil movement characteristics) would chiefly be attributed to the variability in system damping (again, focused in the foundation and SSI). Reasonable estimates of the COV associated with this effect on the earthquake loadings in the primary structure elements of a GBS platform would be in the range of COV = 0.3 to 0.4 (consistent with the variability in the soil damping and SSI interaction characteristics).

15

3.3 Hydrodynamic Effects

The distribution of mass for horizontal excitations along the heights of a typical steel, template-type platform and a concrete GBS platform is shown in Fig. 3.7. Unlike the steel, template-type platform mass of the GBS is concentrated at its base. This mass is primarily associated with hydrodynamic effects (water inside, and motion pressures outside). The realistic characterization of this mass is an important part of determining earthquake loadings induced in a concrete GBS.

There are two hydrodynamic effects of concern. The first is associated with the accelerations of the GBS and the hydrodynamic pressures that are developed by these accelerations. The second is associated with the wave making, viscous drag, and the associated energy dissipation characteristics (damping) developed by the relative motions of the structure and water.

The issues associated with the hydrodynamic effects associated with the GBS accelerations have been addressed by a variety of investigators for a variety of applications including dams (Liaw, Chopra, 1973), reservoir intake towers, bridge support piers, and concrete GBS platforms (Garrison, Berklite, 1972, Liaw, Reimer, 1975).

Results from the analytical and experimental study of hydrodynamic masses associated with the horizontal acceleration of surface piercing cylinders published by Liaw and Reimer (1975) are summarized in Fig. 3.8. The common assumption is that the 'added' mass is equal to the displaced volume. These results indicate that this would be very conservative for GBS whose diameter were about equal to the water depth (e. g. the Hibernia GBS, Bea, 1990). These results indicate that the added mass would be about 50 % of the displaced volume. This difference would equate to an error of two in the computed horizontal loadings associated with a given earthquake acceleration. The effect is significant for cylinder geometries that would be associated with the supporting towers of GBS. For typical tower gometries, the added mass would be 70 to 80 % of the displaced volume of the tower. Note that the added mass at the free surface must be zero (atmospheric pressures).

Fig. 3.7 - Distributions of Horizontal Motions Mass

Fig. 3.8 - Hydrodynamic Mass Distribution

Damping in concrete dam intake towers has been considered by Liaw and Chopra (1973). Pluck tests on the towers with the reservoirs at a low level indicated damping ratios at low strains in the range of 2 % to 4 % of critical. When the reservoirs were flooded, the damping ratios dropped to 1 % to 2 %. The drop in the damping ratio was due to the increase in the critical damping coefficient caused by the increased mass associated with the intake tower vibrating in water. The majority of the damping associated with the hydrodynamic interactions of the intake towers was due to wave making by the tower motions near the free surface. Motions at depth below the free surface are not large enough to develop significant fluid flow separation and hence drag-type (velocity dependent) damping.

Byrd (1978) has studied the hydrodynamic added masses and damping associated with deeply submerged circular tanks similar to those that form the gravity bases for GBS (Fig. 3.4) subjected to
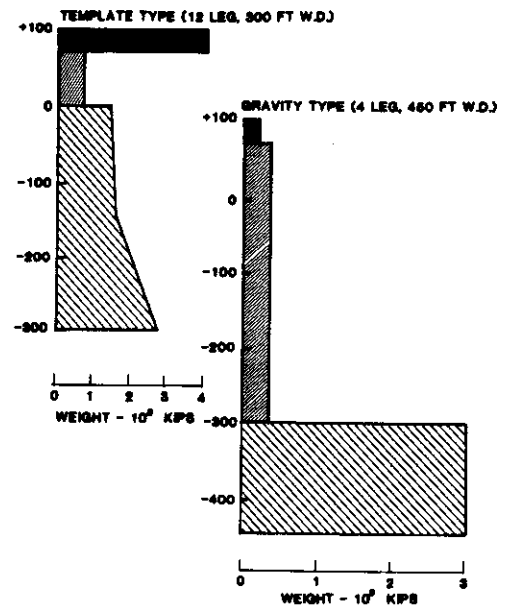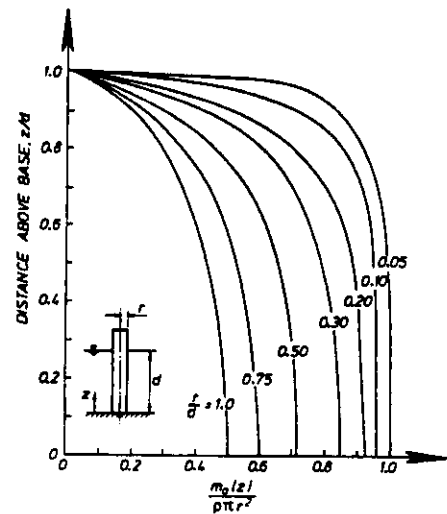
16

earthquake excitations. Measured hydrodynamic damping ratios for horizontal motions ranged from 0.8 % to 1.8 % and those for vertical motions ranged from 0.7 % to 4.4 %. Damping for rocking motions ranged from 0.3 % to 1.2 %. For deeply submerged circular tanks, the added mass coefficients were 0.52, 0.62, and 0.24 for horizontal, vertical, and rocking modes. Byrd found excellent agreement between the measured and diffraction theory based values of added masses. As the top surface of the GBS base nears the free surface, there is a reduction in the added mass coefficients. The decrease starts at a depth below the free surface equal to about 2 times the GBS base height (similar to the decrease indicated in Fig. 3.9). When the GBS base has a water depth over its top surface equal to its height, the added mass for horizontal motions is equal to 0.35 as compared with 0.52 for a water depth of 3 times the GBS height. The experimental data indicated coefficients of variation in the added mass coefficients in the range of 15% to 20 %.

In development of the ISO guidelines for design of concrete GBS, it will be very important to prescribe how hydrodynamic damping and mass effects should be accounted for.

Given these developments, the median bias in the computed earthquake forces could range from B_S = 1.0 to 0.5. The B_E = 1.0 would be associated with the use of sophisticated diffraction theory methods to determine the hydrodynamic interaction related masses and damping. The B_E = 0.5 would be associated with the use of the assumption that the hydrodynamic added mass is equal to the displaced volume and that the hydrodynamic damping is negligible (Bea, 1990).

3.4 Measured and Predicted GBS Motions

There have been some comparisons of measured and predicted responses of GBS nuclear power plant structures (Bechtel Group Inc., 1988). The study performed by Bechtel for the Electric Power Research Institute (EPRI) was performed utilizing forced vibration test data from a nuclear power plant in Japan. The objective of the study was to evaluate the validity of the lumped parameter SSI model that is currently adopted in the U. S. nuclear industry for seismic SSI analyses. The analytical method followed the response spectrum based - frequency domain - discrete element and impedance approach discussed earlier for offshore concrete GBS. The structure - foundation model for this nuclear power plant was identical to the response spectra based analytical model discussed earlier (Fig. 2).

Two foundation models were evaluated. One employed equivalent springs and dashpots at the base
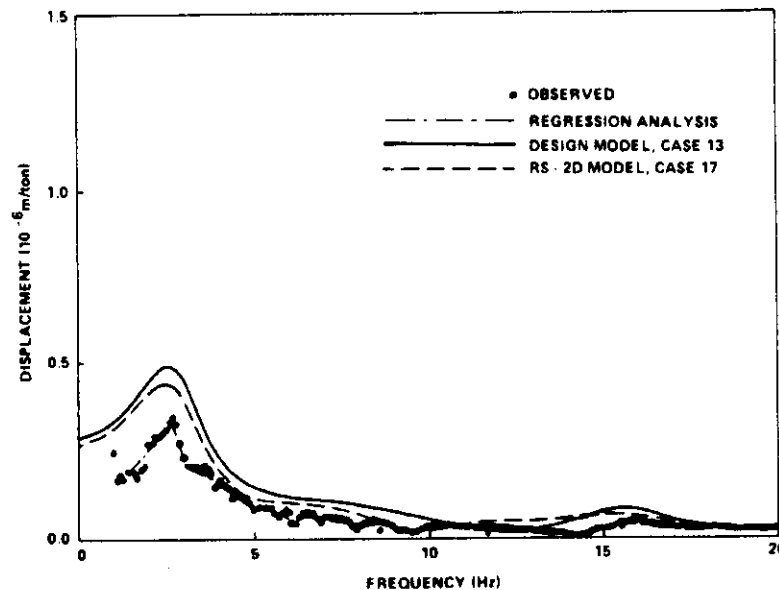

Fig. 3.9 - Comparison of Measured and Computed Displacements

of the structure to simulate the foundation stiffness and damping. The other employed the off-diagonal coupling terms (impedance approach). The lumped parameter models considered both frequency independent and frequency dependent foundation impedances (stiffness and damping for modes of motion). Results from very high quality geotechnical and geophysical studies were used to characterize the soil properties, layering, and variation of soil parameters.

Results from one of the tests compared with the predicted results based on the 'design model' is shown in Fig. 3.9. At high frequencies (above about 5 Hz), generally there is very good agreement between the measured and predicted results. However, in the frequency ranges associated with the lateral responses of offshore concrete GBS platforms, the agreement is not as good. Generally the design model provides a conservative evaluation of the maximum displacements. The bias indicated by the comparisons of measured and predicted responses are in the range of $B_E = 0.5$ in the low frequency range (frequencies less than 1 to 2 Hz) and in the range of $B_E = 1.0$ to 0.9 in the high frequency range (frequencies greater than 5 Hz). There are small differences between the design model that employed sophisticated impedance functions to simulate the foundation response characteristics and the two dimensional response spectra model that employed discrete elements to simulate the foundation response characteristics.

It should be noted that these were relatively low amplitude vibrations in which significant nonlinear effects in either the superstructure or foundation were not present. However, one would expect to be able to achieve the best agreements between the predictive models and the measurements for these low amplitude - strain conditions. Soil - foundation damping controls the magnitude of the first peak in the response spectra at a frequency of about 3 Hz. The analytical comparisons consistently indicated that more damping in the soil - foundation system than was evaluated for the analytical models. The frequency of the predicted first peak closely matches that measured; thus indicating that the foundation masses and stiffnesses were closely predicted.

Based on the results from this extensive series of tests and analyses, it is apparent that the single most important aspect of simulating the performance characteristics of a GBS is that of simulating the soil - foundation interactions with the most important and difficult to determine accurately factor being damping. The evaluation of the appropriate masses and stiffnesses associated with the foundation interactions appears to be much more straightforward.

As was concluded in Section 3.2, the comparisons of measured and response spectra predicted GBS motions (reflecting effective forces) indicates median Biases in range of $B_E = 0.5$ in the low frequency range of primary
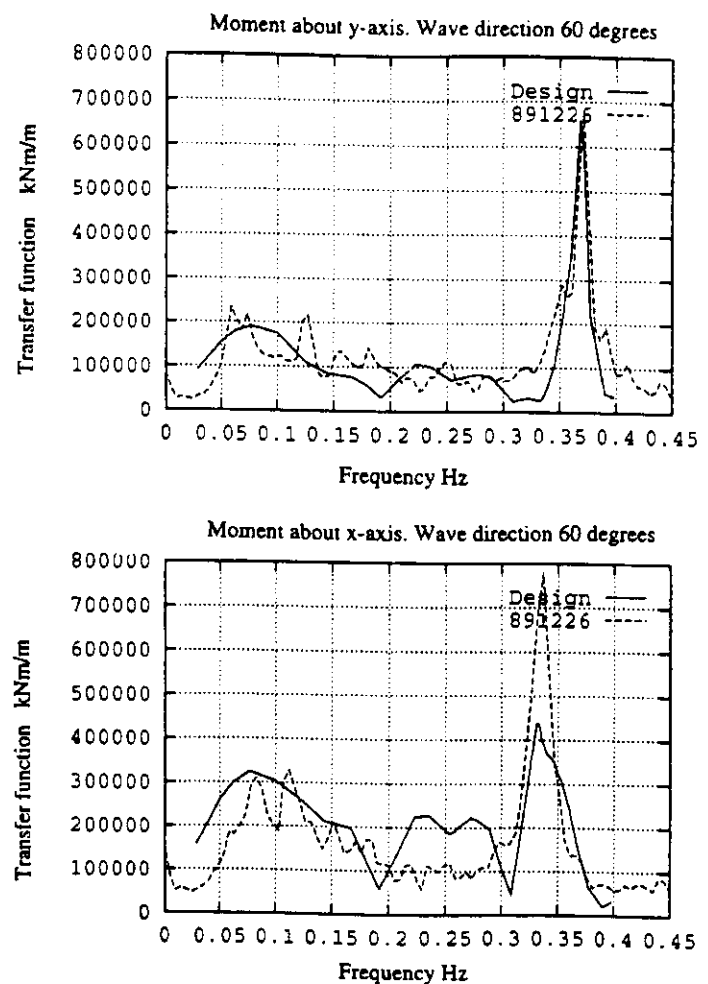

Fig. 3.10 - Measured and calculated GBS transfer functions

18

interest. However, in the high frequency range, the median biases are much closer to unity. Thus, in this development resulting earthquake loading median biases in the range B_E = 1.0 to 0.5 will be evaluated.

Fig. 3.10 summarizes results from measurements and predictions of a North Sea concrete GBS (Gullfaks C) response characteristics (Langen, Skjastad, Haver, 1997). Measured and design wave loading transfer functions for the moments in the support shafts at the top of the GBS base are shown. The analytical model used to develop these transfer functions was identical to the spectral analysis model discussed earlier in this Chapter (Fig. 3.3, Fig. 3.4) (DNV, 1982).

In general there is reasonably good agreement between the predicted and measured transfer functions. The natural period of the platform was measured as 3.0 sec; the design natural period was 3.5 sec. The measured system damping ratios for horizontal bending motions ranged from 1.4 % to 1.6 %. It was observed by the authors that these damping ratios were higher than those assumed in design (for wave loadings). It is encouraging that the response periods and mode shapes were accurately predicted. The authors observed that the soil stiffness that was based on the measured platform responses was higher than assumed in design. The stiffnesses inferred from the measurements were a factor of 1.25 to 1.8 for the horizontal translation base movements.

this page left blank intentionally

Chapter 4

Capacity and Ductility Considerations

4.0 Introduction

The following concrete GBS elements ultimate limit state capacity and ductility considerations were reviewed during this study:

1) Flexural / shear capacity characteristics of concrete GBS columns (support shafts),

2) Caisson cells that comprise the GBS base (domes, shear walls)

2) Base mat sliding characteristics.

In this study, the reference guideline for design of the concrete elements was taken to be Norwegian Standard NS 3473 (1992) and the Det Norske Veritas (DNV) guidelines for design of concrete structures (DNV, 1980a). The reference guideline for design of the foundation elements was taken to be that issued by Det Norske Veritas (DNV, 1980b).

4.1 Concrete Support Shafts

Previous studies of the earthquake response and performance characteristics of concrete GBS structures subjected to earthquake excitations have indicated that the critical structural elements are the columns or support shafts and the steel deck section support structure (Fig 3.2) (Watt, et al, 1978, Norwegian Contractors, 1981; Panel on Offshore Platforms, 1980; PMB Systems Engineering Inc., 1984).

Moan (1995) has summarized the uncertainties of material and geometric properties relevant for offshore concrete structures and the model uncertainties for resistances of concrete beams. These results are summarized in Table 4.1 and Table 4.2.

Table 4.1 - Uncertainties in properties relevant for offshore concrete structures

| Property	Bias	COV	References
concrete compressive strength	1.1	0.10	Haug, Jakobsen, 1990
concrete tensile strength	1.2	0.15	Petkovic, et al, 1992
Reinforcement yield stress	1.12.	0.06	Petkovic, et al, 1992
Prestressing wire strength	1.06	0.04	Petkovic, et al, 1992
Concrete wall thickness			
- walls	1.0	0.05	Petkovic, et al, 1992
- domes	1.0	0.11	Petkovic, et al, 1992
Distance between tensile compressive longitudinal reinforcement	0.95	0.05	Moan, et al, 1991
Location of shear reinforcement	1.00	0.10	Moan, et al, 1991

Table 4.2 - Model uncertainties for capacities of concrete beams

Loading	Material	Bias	COV	Reference
Bending	normal density aggregate	1.13	0.10	Petkovic, et al, 1992
	light weight aggregate	1.27	0.12	Petkovic, et al, 1992
Shear w/o reinf. w reinf. w/ axial comp. & w/o reinf.		1.48 1.23 1.22	0.41 0.35 0.24	Petkovic, et al, 1992 Petkovic, et al, 1992 Petkovic, et al, 1992

Review of the references cited by Moan (1995) indicates that the testing to define these characteristics were at specified 'static' loading rates. The beam capacity tests were referenced to cylinder and cube strength tests performed on the concrete used in fabricating the beams. Strength was determined at 14 days.

Given that the concrete fabricator controlled the strength of the concrete so that only 5 % of the concrete samples tested would fall below the designated design concrete strength and that the concrete had a coefficient of variation of 10 %, one could expect a bias on the static compressive strength of 1.2 (Table 4.1). The bias on the shear capacity of the beams with shear reinforcement would be 1.2. The resultant bias on the fabricated beams would be 1.4. This bias does not include the increase in the strength with aging and with increased strain rates.

Fig. 4.1 shows the COV of concrete compressive strength (14 days) for current high quality concrete construction methods (LaFraugh, 1987, CSA, 1989a; Haug, Jakobsen, 1990; Moksnes, Jakobsen, 1985). There is a trend of decreasing COV with increased compressive strength. This makes sense since higher quality assurance and control procedures are generally used for the very high concrete strength mixes. The high strength compressive strength COV's are comparable with modern steel tensile strength COV's.
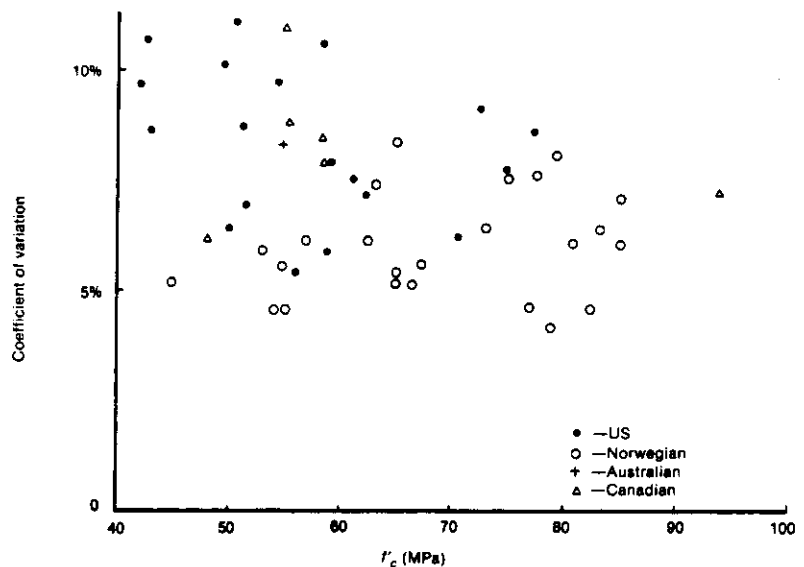
Fig. 4.1 - COV of concrete strength (14 days)

Capacity characteristics of concrete elements characteristic of those used in construction of nuclear power plants (containments, shear walls, columns) have been developed by Hwang, Reich, Ellingwood and Shinozuka (1986). Their analysis of test data from nuclear power plant construction indicated a mean (median) concrete strength in situ that was 1.22 times the nominal strength. The variability of in situ strength (Normally distributed) had a COV of 14 %.

Table 4.3 summarizes the mean ratios of ultimate capacity to nominal capacity (R_{50} / R_n) for the concrete elements (based on ACI /NRC guidelines and test compressive strengths), and the COV's associated with these capacities. Note that precast, pretensioned concrete elements have a COV that is

22

generally smaller than the cast-in-place post-tensioned elements. This reflects the better quality control and working conditions associated with the precasting operations (MacGregor, 1983). Also, note that for the cast-in-place post tensioned elements that the bias and uncertainty are a function of amount of reinforcement and post-tensioning in the elements. The high side of the ranges shown in Table 4.3 for these elements is associated with dense reinforcement and large amounts of post-tensioning. These values are consistent with those used in development of a probability based load criterion for the American National Standard A58 (Ellingwood, Galambos, MacGregor, Cornell, 1980; Ellingwood, Ang, 1972; Holand, 1976).

Table 4.3 - Concrete element capacity characteristics

Elements	Loadings	R_{50} / Rn	COV
Reinforced Slabs	Flexure, Pressure	1.12 - 1.22	0.14 - 0.16
Reinforced Beams	Flexure	1.01- 1.09	0.11 - 0.12
Prestressed Precast Beams	Flexure	1.04 - 1.06	0.057-0.097
Post-tensioned Cast-in-Place Slabs, Domes	Flexure, Pressure	1.02-1.05	0.061-0.144
Short Columns	.	0.95 - 1.05	0.14 - 0.16
	Axial and	.	
Slender Columns	Flexure	0.95 - 1.10	0.17-0.12

Tests of scaled GBS concrete support shafts have been performed by Whittaker (1987). These columns were subjected to axial and flexural static and cyclic loadings. Fig. 4.2 summarizes the results of a comparison of the 'overstrength factor' (test capacity / predicted capacity = Bias) as a function of the axial stress. For 'typical' axial stress ratios (0.1 to 0.2), the median bias is about 1.1 The test data indicate a COV of about 15 %. These data were compared with results provided by Suharwardy and Peknold (1978) and good agreement was indicated.

Results from one of the cyclic lateral loaded column tests is shown in Fig. 4.3. The column was able to develop a peak lateral loading capacity that was about 1.3 times the predicted design capacity. The column was able to develop a ductility of about 12 in repeated cyclic loadings to the peak lateral loading capacity without substantial reductions in the capacity of the column. The predicted peak design capacity was based on the measured strength of the concrete. The loading rates were comparable with standard 'static' testing rates.

Recently, results from lateral and axial loading tests on circular columns (concrete bridge piers) have become available (Kunnath, E-Bahy, 1998). These tests employed earthquake-type cyclic loadings, current concrete quality assurance and control measures, and current earthquake design guidelines that require large amounts of circumferential
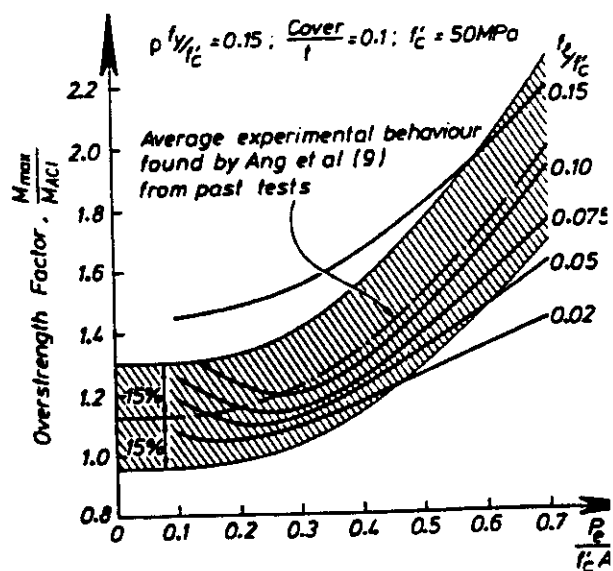
Fig. 4.2 - Comparison of predicted and experimental moment capacities

reinforcement to assure containment of the concrete during intense loadings. Fig. 4.4 summarizes results from one of the tests. The results are very similar to those developed by Whittaker. The columns developed lateral loading capacities that were in the range of 1.1 to 1.2 times those based on the design analysis and the nominal concrete strengths. The columns were able to develop ductilities (ratio of displacement at collapse to elastic displacement) in the range of 4 to 5 and residual strength ratios in the range of 0.9 to 0.8.

These results indicate that a reasonable estimate of the median bias and COV in the earthquake loading capacity of concrete GBS columns is in the range of B_{RE} = 1.2 to 1.4 and COV = 0.10 to 0.15. The earthquake loading expected ductility could be estimated to be in the range of μ = 4 to 6 and the associated residual strength ratio to be in the range of α = 0.75 to 1.0.

Fig. 4.3 - Experimental cyclic lateral load - displacement compared with predicted behavior (Whittaker, 1987)

4.2 Sliding of GBS Mats

Sliding of GBS mats has been studied by a number of investigators (Kraft, Murff, 1975; Young, et al, 1974; Eide, Andersen, 1984; Lacasse, 1992, Golder, 1988; Bea, 1990; Yokel, Bea, 1986). Given the use of current methods to determine bearing, sliding, and overturning capacities, this mode of performance has been found to be the critical mode of performance for most GBS platform foundations.

The sliding resistance, R, of a GBS mat can be expressed as (Thompson et al, 1986; Canadian Standards Association, 1989b):

Fig. 4.4 - Experimental cyclic lateral load - displacement compared with predicted behavior (Kunnath, El-Bahy, 1998)

R = Su A + W tan ϕ'

where Su is the effective undrained shear strength along the sliding zone, A is the area of the sliding zone, W is the vertical weight on the foundation, and ϕ' is the effective value of internal friction of the soil in the sliding zone. All of these parameters can be interpreted as random variables (Lacasse, 1992).

For a cohesive soil, Su will dominate the resistance (undrained behavior). For a cohesionless soil, ϕ' will dominate the resistance. Both soil parameters will be influenced by the presence of the structure (e.g. vertical stress increasing strength) and the characteristics of the loadings (cyclic loadings leading to decreases in strength, high rates of loading leading to increases in strength). The SSI influences the soil characteristics (near-field soils) and the soil characteristics are influenced by the earthquake (free-field soils). The area of the sliding zone can be influenced by the foundation geometry and the soil characteristics. The weight on the foundation is also variable.
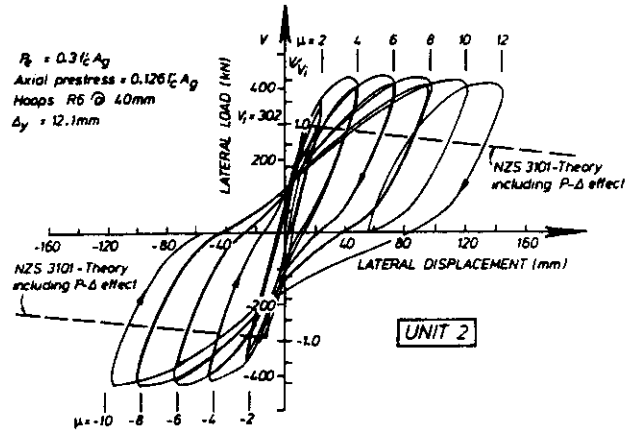
24

The basic soil characteristics will depend greatly on how the soils are sampled or tested in situ, how the samples are preserved, how the samples are tested, how the test data is interpreted, and the methods used to analyze the performance of the GBS mat. It is important to note that the majority of these steps result in degrading the strength of the soils; indicating lower effective strengths than in situ during earthquakes.

If modern methods are used to determine the soil characteristics and to perform the analyses of the SSI, then one could expect that the median bias in the predicted sliding capacity would be close to unity. However, if less rigorous methods are used to determine the soil characteristics and to analyze the SSI, then the bias could be in the range of 2 or more. The value of 2 could be developed from a soil boring performed using bumper-subs and drill collars and low controls on drilling mud weight and pressures (x 1.3), wireline sampling techniques (x 1.4), extruded Shelby tube samples (x 1.1), high quality direct simple shear tests (x 1.0), and explicit recognition of structure and earthquake SSI effects (x 1.0). The value of 2 could be developed from a soil boring performed using heave compensation and highly controlled drilling mud weights, viscosities, and pressures (x 1.1), large-diameter push sampling (x 1.1), sectioned tube samples, (x 1.1), unconolidated - undrained triaxial tests (x 0.9), and analysis of the 'static' sliding resistance (x 1.7) (Bea, 1997).

While in situ tests avoid many of the disturbance problems associated with drilling, sampling, packaging, transportation, and laboratory sample preparation and testing, they are not devoid of soil disturbance and interpretation considerations. In situ tests can be performed in such a way that they can lead to either an underestimate or overestimate of the soil strength appropriate for evaluation of GBS mat sliding resistance (Young, et al, 1974; Canadian Standards Association, 1989b).

The best information presently available to evaluate the bias and uncertainty associated with analyses of GBS foundation performance have been provided by data from 1-g and centrifuge model tests (Andersen, et al, 1989a; 1989b; Allard, et al, 1994; Finnie, Randolph, 1994; Watson, Randolph 1997). In the preceding and following developments on GBS sliding characteristics, the unique aspects associated with calcareous soils will not be addressed.

Results from the test series published by Andersen, et al, 1989a, 1989b) on cyclic loading tests on mats supported by cohesive soils are summarized in Fig. 4.5. The two test series shown (a, b) are for two different storm cyclic loading histories. Excellent agreement is developed between the calculated and measured sliding capacities, and there is reasonably good agreement between the calculated and measured displacements. As noted by Andersen, et al, 1989b), the calculated displacements are very sensitive to some of the assessments that must be integrated into the analyses (the effects of one of these is shown in Fig. 4.5b). The sophisticated SSI model developed by Andersen, et al (1989a) were used to develop the evaluations of mat load - displacement characteristics.

The recently published work on GBS sliding capacities in cohesionless soils (Andersen, Allard, Hermstad, 1997) indicates that the sliding capacity of these foundations is considerably more complex than that of mat sliding capacities in cohesive soils. The results of this test series on dense sands indicates that a horizontal force could be exerted on the mat for more than a wave period that was 1.95 times the mat weight. A cyclic horizontal load of more than 1.35 times the mat weight could be exerted during the cyclic tests without developing large lateral displacements. These two values indicate an effective value of internal friction in the dense sands of 63° and 53°, respectively. The friction angle from the triaxial tests was 40.3° for undrained conditions and 44.5° for drained conditions. The large horizontal loads could be resisted because the very dense sands dilated strongly when sheared and because the foundation remained essentially undrained during the loading cycles. The authors note that the test horizontal loads are considerably higher than the characteristic maximum horizontal load of 0.33 to 0.41 times the mat weight which is typical for existing North Sea GBS. A very large bias on the characteristic design sliding capacity is indicated. Sliding capacity loads calculated with the assumption that dilatency effects can not be relied upon were less than 50 % of the applied loads. Biases in the range of 2 (minimum) to 4 are indicated.
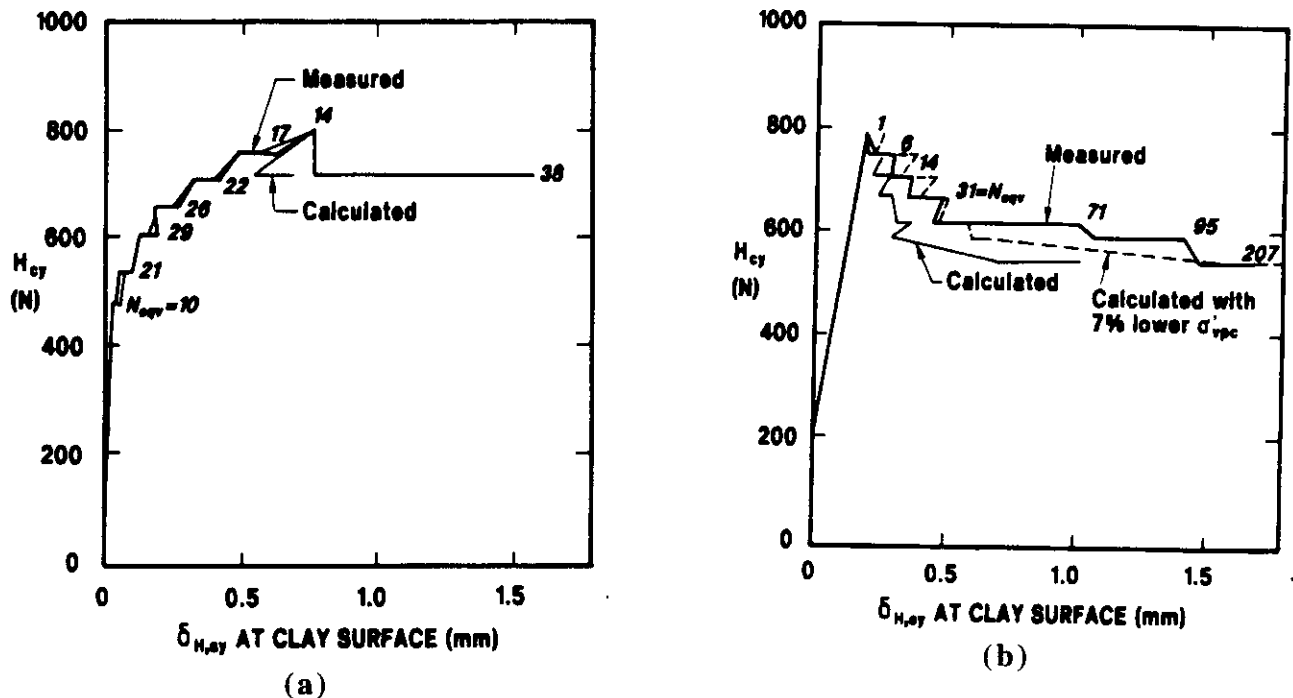
Fig. 4.5 - Calculated and measured cyclic horizontal mat loadings and displacements

Present guidelines to determine GBS mat sliding capacities are not sufficiently detailed to allow a general specification of the bias and uncertainties. Specification of biases will need to be closely correlated with the specific methods used to sample, test, and analyze the soils and the earthquake SSI. Consequently, median biases in the range of B_{RE} = 1.0 to 3.0 will be used in these developments. The only way to reduce this range is to develop very specific guidelines that will address the critical aspects of development of assessments of GBS mat sliding capacity.

Evaluation of the natural uncertainties (Type I) in the sliding capacity is somewhat more straightforward. The majority of this uncertainty is associated with the natural variabilities in the soil characteristics and the influences of the structure and earthquake SSI on the natural variabilities (Kraft, Murff, 1975; Golder Associates, 1988; Bea, 1990). For soil conditions in which the behavior during earthquakes is primarily undrained, this natural variability is estimated to be in the range of COV = 0.3 to 0.4 (Golder Associates, 1988). For soil conditions in which the behavior during earthquakes is primarily drained, this natural variability is estimated to be in the range of COV = 0.4 to 0.5 (Golder Associates, 1988).

The ductilities that can be developed by GBS mat sliding are fundamentally limited by appurtenances that are attached to or contained in the GBS that penetrate into the underlying foundation soils or are supported by the sea floor soils (e.g. risers, well conductors). These ductilities could be estimated to lie in the range of μ = 10 to 12 (Thompson, et al, 1986; Bea, 1990). The sliding resistance residual strength factor could be estimated to lie in the range of α = 0.7 to 0.9 (Fig. 4.5).

26

Chapter 5

Loading Effects Considerations

5.0 Introduction

The loading effects factor, Fe, is intended to include the effects of nonlinear behavior of a structure system in the elastic design response spectrum. Previously, the median loading effects factor for earthquake loadings was expressed as:

$$\mathbf{Fe} = \mu \; \alpha^{-1} \dotfill (5.1)$$

where μ is the ductility, and α is the residual strength factor (Appendix B). The analyses on which this relationship were developed indicates a COV around the median loading factor in the range of COV = 30 % to 40 %. This range is due to the differences in the characteristics of the earthquakes that were used to study the responses of the nonlinear systems. This source of variability has been previously included in the characterizations of earthquake ground motions at the platform location (σ_{SE}, , σ_{GS}).

The background developed in this report indicates that for the concrete columns - support shafts, μ = 4 to 6 and α = 0.75 to 1.0, and for the GBS mat sliding, μ = 10 to 12 (as controlled by interactions with appurtenances), and α = 0.8 to 1.0. On a very stiff foundation, the GBS system ductility and residual strength characteristics would be controlled by the support columns. On a very soft foundation, or for a GBS with very short and strong support columns, the system ductility and residual strength characteristics would be controlled by the mat - appurtenances interactions.

The purpose of the review conducted during this study was to determine if there should be any modifications to the above expression due to the unique performance characteristics (e.g. cyclic strength and stiffness degradation) of concrete GBS platform systems (e.g. Figs. 4.3 and 4.4).

5.1 Loading Effects Factors

Miranda (1994) has published results of an extensive study of the responses of bilinear elasto-plastic (α = 1.0) single degree of freedom (SDOF) systems. This study involved a study of 124 earthquake ground motion time histories recorded on a wide range of soil conditions and for a wide range of seismotectonic conditions. The results indicated:

$$\bullet \; Fe = \Phi / \mu - 1 \dotfill (5.2)$$

$$\bullet \; \text{rock sites} - \Phi = 1 + 1 / (10T - \mu T) - (1 / 2T) \exp[-3/2(\ln T - 3.5)^2] \dotfill (5.3)$$

$$\bullet \; \text{alluvium sites} - \Phi = 1 + 1 / (12T - \mu T) - (2 / 5T) \exp[-2(\ln T - 1/5)^2] \dotfill (5.4)$$

The resulting Fe's for rock and alluvium sites are shown in Fig. 5.1 and Fig. 5.2 as a function of the period, T, and the ductility. The relationship used in the proposed LRFD development is a very good approximation to these results for periods greater than about 0.5 sec. Fe is underestimated for periods less than 1 sec.

Al-Sulaimani and Roessett (1984) conducted a similar study of stiffness and strength degrading systems. Their results were interpreted as a correction factor to the results developed by Miranda for elasto-plastic, non-degrading systems. Al-Sulaimani developed strength and stiffness degradation parameters characteristic of concrete columns (Fig. 4.3, Fig. 4.4). The correction factor is a function of the ductility and the period range. Their results are summarized in Fig. 5.3. The residual strength factor used in the proposed ISO criteria is a very good approximation to the results for the degrading concrete elements in the long period range for $\alpha \approx 0.8$ to 0.9.

Given concrete GBS support shafts $\mu = 4$ to 6 and $\alpha = 0.75$ to 1.0, and for the GBS mat sliding, $\mu = 10$ to 12 (as controlled by interactions with appurtenances), and $\alpha = 0.8$ to 1.0, these results indicate that the effective loading factors would lie in the range of $Fe = 0.11$ to 0.33.
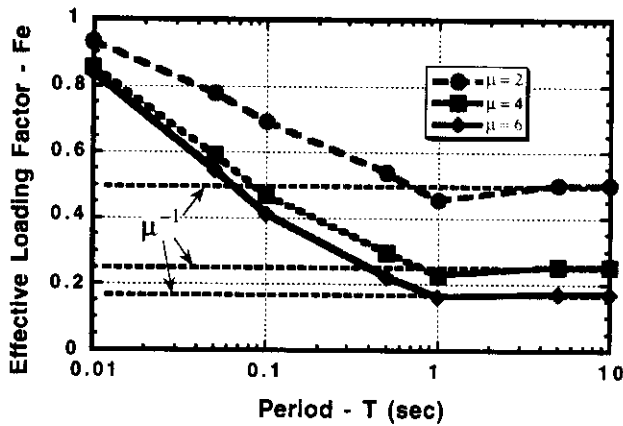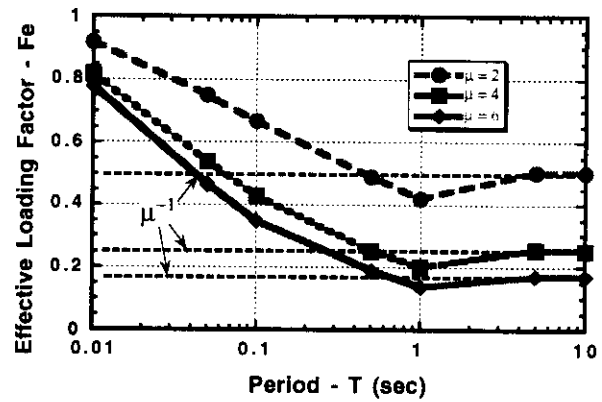

Fig. 5.1 - Loading effects factors for rock sites
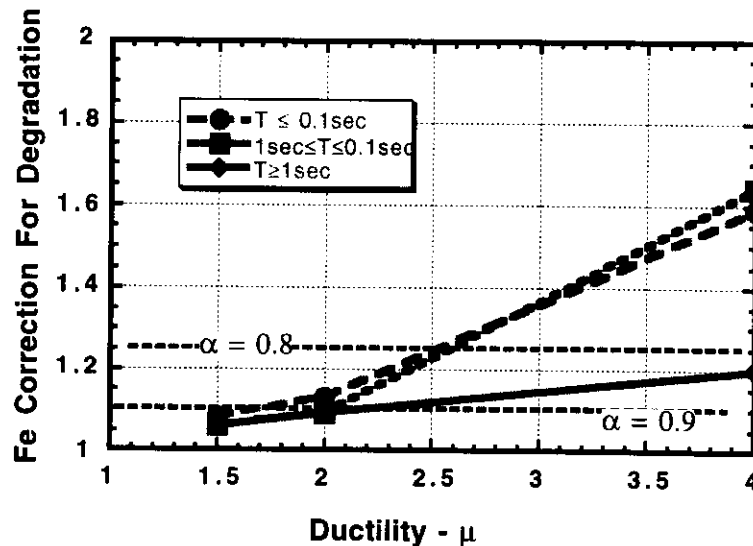
Fig. 5.2 - Loading effects factors for alluvium sites

Fig. 5.3 - Correction for stiffness and strength degrading systems

Loading & Resistance Factors

6.0 Introduction

Given the foregoing developments, reliability based earthquake loading and resistance factors can be developed for the concrete GBS elements included in this study.

6.1 Earthquake Loading Factors

Reliability based earthquake loading factors can be determined from:

$$\gamma_E = Fe \; B_E \; \exp (0.8 \; \beta_E \; \sigma_E - 2.57 \; \sigma_E) \quad\dots\dots\dots\dots\dots\dots\dots\dots\dots\dots\dots\dots\dots\dots\dots\dots\dots (6.1)$$

This study has indicated the following key components for concrete GBS:

Fe = 0.21 to 0.33 (support shafts shear/flexure) and 0.11 to 0.12 (mat sliding)

B_E = 0.5 to 1.0 (depending on details of the response spectra analyses and location in structure)

σ_{RS} = 0.3 to 0.4 (depending on natural variabilities in SSI energy dissipation characteristics)

The loading factors developed here are referenced to a 200-year average return period median elastic response spectrum. If it were desired to utilize comparable 100-year earthquake characteristics, then the loading factors would need to be multiplied by a factor:

$$Z = \exp (0.24 \; \sigma_E) \quad\dots\dots\dots\dots\dots\dots\dots\dots\dots\dots\dots\dots\dots\dots\dots\dots\dots\dots\dots\dots\dots (6.2)$$

The annual Safety Indices for the earthquake loadings (β_E) will kept the same as those used to develop the proposed ISO guidelines for steel, template-type platforms (Appendix B, Table 1). Three 'Serviceability and Safety Classes' (SSC) are defined: SSC 1, $\beta_E = 2.3$; SSC 2, $\beta_E = 3.0$, and SSC 3, $\beta_E = 3.7$.

Depending on the seismic zone classification, the uncertainties (standard deviation of the logarithms of the annual maximum earthquake ground motions) associated with the seismic sources and earthquake attenuation ranged from $\sigma_{SE} = 1.0$ to 2.0. Depending on the local soil and geology classification, the uncertainties associated with the local site and geology effects ranged from $\sigma_{GS} = 0.3$ to 0.5. The resultant uncertainties for these components equates to $\sigma_E = 1.09$ to 2.10. It is clear that the natural uncertainties associated with the seismic sources and earthquake attenuation dominate the natural uncertainties in the concrete GBS loading effects (Fig. 1.4)

Based on a 'conservative' application of these developments with **Fe** = 0.35, $B_E = 1.0$, and $\sigma_{RS} = 0.4$, Table 6.1 summarizes earthquake loading factors for each of the three SSC as a function of the four categories of seismic sources (Appendix B, Table 6) for site classifications SC-B and SC-D (stiff soils, Appendix B, Table 3).

Ductility Level Earthquake (DLE) average return periods that would be used to demonstrate adequate capacity and ductility in the concrete GBS would be 1,000 years and 10,000 years for SSC

#2 and #3, respectively. These return periods are the inverse of the annual probabilities of failure associated with the platform SSC (refer to Step #8 in Appendix B).

Most concrete GBS in the North Sea would be identified as SSC 3, the seismotectonic classification would be Type D, and the resulting load factor would be $\gamma_E = 0.79$.

Table 6.1 - Concrete GBS earthquake loading factors for strong alluvium site soil conditions

SSC	Type Seismic Source			
	A	B	C	D
1	0.15	0.12	0.13	0.08
2	0.42	0.27	0.28	0.25
3	0.55	0.63	0.58	0.79

6.2 Earthquake Resistance Factors

Reliability based earthquake resistance factors can be determined from:

$$\phi_E = B_{RE} \exp(-0.8 \, \beta_E \, \sigma_{RE}) \dots\dots\dots\dots\dots\dots\dots\dots\dots\dots\dots\dots\dots\dots\dots\dots\dots\dots\dots(6.3)$$

Based on available test data, the GBS concrete support shafts are estimated to have median capacity biases for earthquake loadings in the range of $B_{RE} = 1.2$ to 1.4 and COV = 0.10 to 0.15 (Fig. 4.3, Fig. 4.4). These biases are based on referenced to the design or nominal 14-day concrete compressive strength, to the nominal steel yield strengths, and to intense earthquake loadings. A 'conservative' median bias of $B_{RE} = 1.2$ and COV = 0.15 will be used in development of the loading factor for the support shafts.

The GBS mat cast-in-place post-tensioned domes and shear wall silos are estimated to have median capacity biases for earthquake loadings in the range of $B_{RE} = 1.1$ to 1.3 and COV = 0.06 to 0.14 (Table 4.3). A 'conservative' median bias of $B_{RE} = 1.1$ and COV = 0.15 will be used in development of the loading factor for the GBS base mat components (slabs, domes, shear walls, connections).

The GBS mat earthquake sliding capacities are estimated to have capacity median biases in the range of $B_{RE} = 1.0$ to 3.0, COV = 0.3 to 0.4 for undrained soil loading conditions, and COV = 0.4 to 0.5 for drained soil-loading conditions. A 'conservative' median bias of $B_{RE} = 1.0$ and COV = 0.4 for undrained and $B_{RE} = 2.0$ and COV = 0.5 for drained soil loading conditions will be used in development of the loading factor for the GBS base mat sliding.

Table 6.2 summarizes the resulting loading factors for the primary structural elements that comprise a concrete GBS.

Table 6.2 - Concrete GBS element loading factors

GBS Component	SSC 1	SSC 2	SSC 3
Support Shafts	0.91	0.84	0.77
Base Slabs, Shear Walls, Domes	0.83	0.77	0.71
Base Sliding undrained	0.48	0.38	0.31
drained	0.80	0.60	0.46

The 'static' Reserve Strength Ratio (RSR) is a global factor of safety for the concrete GBS structure - foundation system. The RSR is the ratio of the lateral loading at ultimate limit state to the design loading. A reliability based RSR can be determined from:

$$RSR = Fe \ (\ \mathbf{B_E} \ / \ \mathbf{B_{RE}} \ ) \ exp \ (\ \beta \ \sigma - 2.57 \ \sigma_E \ ) \ \dots\dots\dots(6.4)$$

where σ is the resultant uncertainty in the seismic loading effects and the platform seismic loading capacity:

$$\sigma^2 = \sigma_E^{\ 2} + \sigma_{PC}^{\ 2} \dots\dots\dots(6.5)$$

This RSR is based on the design loadings determined from a 200-year return period median elastic response spectrum. If comparable 100-year conditions were used, then the RSR's would need to be increased by the factor indicated in Eqn. 6.2.

This RSR is based on 'best estimate' characteristics and properties in the platform elements and components; the lateral loading capacity that is referenced is the 'actual' median (50 %tile) lateral loading capacity with all median biases set to unity.

Table 6.3 summarizes the RSR's for the four seismotectonic source types, firm alluvium soil conditions, and two SSC (SSC 1 not required to demonstrate ductility) based on a platform seismic loading capacity median bias and uncertainty of $\mathbf{B_{RE}}$ = 1.2 σ_{PC} = 0.15 (associated with correlated failure mode in the GBS supporting columns), a seismic loading median bias of $\mathbf{B_E}$ = 1.0, and a median effective loading factor of $\mathbf{Fe}$ = 0.35. These RSR's are referenced to the 200-year SLE loadings. These RSR's are indicative of the GBS system nominal 'factors-of-safety.'

Table 6.3 - Static reserve strength ratios

SSC	Type Seismic Source			
	A	B	C	D
2	0.5	0.6	0.5	0.7
3	1.1	1.7	1.4	3.2

this page left blank intentionally

Chapter 7

Summary,
Conclusions & Recommendations,
Acknowledgments

7.0 Summary

Reliability based earthquake LRFD guidelines for concrete GBS have been developed using the format used to develop similar LRFD guidelines for steel, pile-supported template platforms. This format has 'information sensitivity' in that it is able to accommodate natural and model uncertainties associated with different regions, structure types, and components.

Available data have been used to characterize the biases and uncertainties associated with the earthquake conditions, characteristics, induced loadings, and loading effects. Available data have been used to characterize the biases and uncertainties associated with the capacities of concrete GBS components when subjected to earthquakes.

For concrete GBS located in the North Sea, the load factor for SSC 3 structures is indicated to be $\gamma_E = 0.79$. This load factor is referenced to a median 200-year average return period elastic response spectrum. This load factor can be compared with a load factor of $\gamma_E = 0.8$ for steel platforms located offshore California and with a load factor of $\gamma_E = 1.1$ for a comparable platform located in the North Sea. The difference in the load factors in the North Sea and offshore California is due primarily to the difference in the uncertainties associated with the annual expected maximum earthquake ground motions in these two regions; uncertainties associated with the earthquake ground motion intensities in the North Sea are a factor of about 2 greater than those offshore California. The difference in the load factors for steel and concrete structures in the same region are due primarily to the differences in the effective loading factors for these two types of structures. These effective loading factors reflect the inherent ductility and residual strength characteristics of these two types of structures.

If 100-year earthquake loading conditions in the North Sea were used as the reference loading condition, the load factor would be increased by a factor of 1.65. The resulting load factor for SSC 3 concrete GBS structures would be $\gamma_E = 1.3$.

For concrete GBS located in the North Sea, the earthquake resistance factors for SSC structures are indicated to be $\phi_E = 0.77$ and $\phi_E = 0.71$ for the GBS support shafts and base mat elements, respectively. These loading factors can be compared with those developed for nuclear power plant concrete shear walls and containments of $\phi_E = 0.65$ for axial compression or flexure with axial compression; this resistance factor is increased linearly from 0.65 to 0.85 as axial compression decreases from 10 % of the gross section compressive strength to zero. The comparable load factor for steel structure diagonal braces subjected to earthquake loadings would be $\phi_E = 1.0$. The differences in loading factors for the concrete elements are due principally to the differences in the capacity biases in these elements. The differences in loading factors for steel and concrete structures reflects this same source; differences in the capacity biases associated with earthquake loadings.

concrete design, seismic actions on structures, dynamic analysis, and geotechnical - foundation design.

7.2 Acknowledgments

this page left blank intentionally

References

Aki, K. (1988). "Local Site Effects on Strong Ground Motion," *Earthquake Engineering and Soil Dynamics II - Recent Advances in Ground-Motion Evaluation*, American Society of Civil Engineers, New York.

Al-Sulaimani, G., J., and Roessett, J. M. (1984). "Design Spectra for Degrading Systems," Journal fo structural Engineering, Vol. 111, No. 12, American Society of Civil Engineers, New York.

Andersen, K. H., Allard, M. A., and Hermstad, J. (1994). "Centrifuge Model Tests of a Gravity Platform on Very Dense Sand; II Interpretation, *Proceedings Seventh International Conference on the Behavior of Offshore Structures*, Pergamon, Elsevier Science Publishers Ltd., Oxford, UK.

Andersen, K. H., Lacasse, S., Aas, P. M., and Andenaes, E. (1982). "Review of Foundation Design Principles for Offshore Gravity Platforms," *Proceedings of the International Conference on the Performance of Offshore Structures*, Vol. 1, Cambridge, Massachusetts.

Andersen, K. J., et al. (1989a). "Model Tests of Gravity Platforms: I. Description," *Journal of Geotechnical Engineering*, American Society of Civil Engineers, Vol. 115, New York.

Andersen, K. J., et al. (1989b). "Model Tests of Gravity Platforms: II. Interpretation," *Journal of Geotechnical Engineering*, American Society of Civil Engineers, Vol. 115, New York.

Bea, R. G. (1984). "Dynamic Response of Marine Foundations," *Proceedings of the Ocean Structural Dynamics Symposium*, Oregon State University, Corvallis, Oregon.

Bea, R. G. (1991). *Loading and Load Effects Uncertainties*, Report to the Canadian Standards Association, Verification Program for CSA Code for the Design, Construction, and Installation of Fixed Offshore Structures, Project No. D-3, University of California at Berkeley.

Bea, R. G. (1997). "Background for the Proposed International Standards Organization Reliability Based Seismic Design Guidelines for Offshore Platforms," *Proceedings of the Earthquake Criteria Workshop: Recent Developments in Seismic Hazard and Risk Assessment*, 16th International Conference on Offshore Mechanics and Arctic Engineering, Yokahama, Japan, (obtain proceedings from Port and Harbors Research Institute, Yokuska, Japan).\

Bechtel Group, Inc., (1988). *Validation of Soil-Structure Interaction Models Using In-Plant Test Data from Japan*, Electric Power Research Institute, Palo Alto, California.

Bozorgnia, YU. Niazi, M., and Campbell, K. W. (1995). "Characteristics of Free-field Vertical Ground Motion during the Northridge Earthquake, *Earthquake Spectra*, Vol. 11, No. 2, Earthquake Engineering Research Institute, Oakland, California.

Brookhaven National Laboratory (1994). *Technical Guidelines for Aseismic Design of Nuclear Power Plants*, U. S. Nuclear Regulatory Commission, NUREG/CR-6241, Washington, DC.

Byrd, R. C. (1978). *A Laboratory Study of the Fluid-Structure Interaction of Submerged Tanks and Caissons in Earthquakes*, Earthquake Engineering Research Center, Report No. UCB/EERC-78/08, University of California at Berkeley.

Canadian Standards Association (1989a). *Commentary to CSA Standard S474-M1989, Concrete Structures*, Special Publication S474.1-M1989, Toronto, Ontario Canada.

Canadian Standards Association (1989b). *Commentary to CSA Standard S472-M1989, Foundations*, Special Publication S472.1-M1989, Toronto, Ontario Canada.

Crouse, C. B., and McGuire, J. W., (1997). *Site Response Studies for Purpose of Revising NEHRP Seismic Provisions,* Dames and Moore Consultants, Seattle, Washington.

Crouse, C.B., and Quilter, J., (1991). "Seismic Hazard Analyses and Development of Design Spectra for Maui A Platform," *Proceedings of the Pacific Conference on Earthquake Engineering,* Auckland, New Zealand.

Der Kiureghian, A., (1996). "A Coherency Model for Spatially Varying Ground Motions," *Earthquake Engineering and Structural Dynamics,* Vol. 25, John Wiley & Sons, New York.

Det Norske Veritas (DNV) (1980a). *Rules for the Design, Construction and Inspection of Offshore Structures, Concrete Structures,* Hovik, Norway.

Det Norske Veritas (1980b). *Rules for the Design, Construction and Inspection of Offshore Structures, Foundations,* Hovik, Norway.

Det Norske Veritas (1982). *Rules for the Design, Construction and Inspection of Offshore Structures, Dynamic Analysis,* Hovik, Norway.

Dolan, D. K., Crouse, C. B., and Quilter, J. M. (1992). "Seismic Reassessment of Maui A," *Proceedings of the Offshore Technology Conference,* OTC 6934, Society of Petroleum Engineers, Richardson, Texas.

Eide, O., and Andersen, K. H. (1984). "Foundation Engineering for Gravity Structures in the Northern North Sea," *Proceedings of the International Conference on Case Histories in Geotechnical Engineering,* Vol. 4, University of Missouri, St. Louis, Missouri.

Ellingwood, B. R., and Ang, A. H.-S. (1972). *A Probabilistic Study of Safety Criteria for Design,* Dept. of Civil Engineering, University of Illinois, Report UILU-ENG-72-2008, Urbana, Illinois.

Ellingwood, B., Galambos, T. V., MacGregor, J. G., and Cornell, A. C. (1980). *Development of a Probability Based Load Criterion for American National Standard A58 - Building Code Requirements for Minimum Design Loads in Buildings and Other Structures,* National Bureau of Standards, U. S. Government Printing Office, Washington, DC.

Farrar, C.R., and Bennet, J. G. (1988). Experimental Assessment of Damping in Low Aspect Ratio, Reinforced Concrete Shear Wall Structure, Los Alamos National Laboratory, U. S. Nuclear Regulatory Commission, NUREG/CR-5154, Washington, DC.

Finnie, I. M. S., and Randolph, M. F. (1994). "Punch-Through and Liquefaction Induced Failure of Shallow Foundations on Calcareous Sediments," *Proceedings Seventh International Conference on the Behavior of Offshore Structures,* Pergamon, Elsevier Science Publishers Ltd., Oxford, UK.

Garrison, C. J., and Berklite, R. B. (1972). "Hydrodynamic Loads Induced by Earthquakes," *Proceedings of the Offshore Technology Conference,* OTC 1554, Society of Petroleum Engineers, Richardson, Texas.

Golder Associates (1988). *Calibration of Soil Resistance Factors,* Report to the Canadian Oil and Gas Lands Administration, Environmental Protection Branch, Ottawa, Canada.

Harichandran, R. S. (1988). "Local Spatial Variation of Earthquake Ground Motion," *Earthquake Engineering and Soil Dynamics II - Recent Advances in Ground-Motion Evaluation,* American Society of Civil Engineers, New York.

Haug, E. K. and Jakobsen, B., (1990). "In situ and Design Strength for Concrete in Offshore Platforms," *Proceedings of the 2nd International Symposium on Utilization of High Strength Concrete,* University of California at Berkeley.

Heaton, T. H., and Hartzell, S. H. (1988). "Earthquake Ground Motions," *Earth Planetary Science,* London, UK

Holdand, I., (1976). "Ultimate Capacity of Concrete Shells," *Proceedings of the Behavior of Offshore Structures Conference*, Vol. 1, Trondheim, Norway.

Hwang, H., Reich, M., Ellingwood, B., and Shinozuka, M. (1986). *Reliability Assessment and Probability Based Design of Reinforced Concrete Containments and Shear Walls*, Brookhaven National Laboratory, Report to U. S. Nuclear Regulatory Commission, Washington, DC.

Karthigeyan, V. (1996). "ISO Panel 5 Seismic Loading and Response, Draft Concrete Annex," Report to International Standards Organization Panel 5, Health and Safety Executive, London, UK.

Kausel, E. A. M., and Sunder, S. S. (1982). *Review of A. S. Norske Shell's Report NO. 9, Earthquake Analysis for the Condeep T300 at the 31/2 Field*, Confidential Report to Statoil, Stavanger, Norway.

Kraft, L. M., and Murff, J. D. (1975). "A Probabilistic Investigation of Foundation Design for Offshore Gravity Structures," *Proceedings of the Offshore Technology Conference*, OTC 2370, Society of Petroleum Engineers, Richardson, Texas.

Kunnath, S. and El-Bahy, A. (1997). "An Evaluation of Progressive Damage in Reinforced Concrete Circular Bridge Columns," *National Center for Earthquake Engineering Research Bulletin*, Vol. 11, No. 4, Buffalo, New York.

Lacasse, S. (1992). Guidelines for Implementation of Probabilistic Approaches in Geotechnical Design of Offshore Structures," Norwegian Geotechnical Institute Report 514165, Oslo, Norway.

LaFraugh, R. W. (1987). "Design and Placement of High Strength Lightweight and Normal weight Concrete for Glomar Beaufort Sea I, *Proceedings of the Symposium on the Utilization of High Strength Concrete*, Stavanger, Norway, Tapir, Trodheim, Norway.

Langen, I., Skjastad, O., and Haver, S. "Measured and Predicted Dynamic Behavior of an Offshore Gravity Platform," *Proceedings Eighth International Conference on the Behavior of Offshore Structures*, Vol. 3, Pergamon, Elsevier Science Ltd., Oxford, England.

Liaw, C.-Y., and Chopra, A. K. (1973). Earthquake Response of Axisymmetric Tower Structures Surrounded by Water," Earthquake Engineering Research Center, Report No. UBC/EERC-80-12, University of California at Berkeley.

Liaw, C.-Y., and Reimer, R. B. (1975). "Hydrodynamic Interaction Effects on the Cylindrical Legs of Deepwater Platforms," *Proceedings Offshore Technology Conference*, Paper 2324, Society of Petroleum Engineers, Richardson, Texas.

Luco, J. E. and Sotiropoulos, D. A. (1980). "Local Characterization of Free Field Ground Motion and Effect of Wave Passage," Bulletin of the Seismological Society of America, Vol. 70, New York.

MacGregor, J. (1983). "Load and Resistance Factors for Concrete Design," American Concrete Institute Journal, New York.

Martin, G. R., and Dobry, R. (1994). "Earthquake Site Response and Seismic Code Provisions," *National Center for Earthquake Engineering Research Bulletin*, Vol. 8, No. 4, Buffalo, New York.

Miranda, E. (1994). "Evaluation of strength Reduction Factors for Earthquake-Resistant Design," *Earthquake Spectra*, Vol. 10, No. 2, Earthquake Engineering Research Institute, Oakland, California.

Moan, T. (1995). *Safety Levels Across Different Types of Structural Forms and Materials - Implicitly in Codes for Offshore Structures*, SINTEF Structures and Concrete, STF70 A95210, Trondheim, Norway.

Moksnes, J., and Jakobsen, B. (1985). "High Strength Concrete, Development and Potentials for Platform Design," *Proceedings of the Offshore Technology Conference*, OTC 5073, Society of Petroleum Engineers, Richardson, Texas.

Murff, J. D., and Miller, T. W. (1977). "Stability of Offshore Gravity Structure Foundations, *Proceedings of the Offshore Technology Conference*, OTC 2896, Society of Petroleum Engineers, Richardson, Texas.

Newmark, N. M. (1969). "Torsion in Symmetrical Buildings," Proceedings Fourth World Conference on Earthquake Engineering, Vol. II, Santiago, Chile.

Norwegian Contractors (1981). *GBS and Steel Deck Earthquake Analysis Report*, Mobil Exploration Norway Inc., Statfjord Development Project, Phase III Platform, C, Oslo, Norway.

Pais, A., and Kausel, E. (1985). "Stochastic Response of Foundations," Research Report R85-6, Dept. of Civil Engineering, M.I.T., Cambridge, MA.

Panel on Offshore Platforms (1980). "engineering Fixed Offshore Platforms to Resist Earthquakes," Earthquake Engineering and Structural Dynamics Symposium, American Society of Civil Engineers, New York, NY.

Penzien, J., and Tseng, W. S. (1976). "Seismic Analysis of Gravity Platforms Including Soil-Structure Interaction Effects," *Proceedings of the Offshore Technology Conference*, OTC 2674, Society of Petroleum Engineers, Richardson, Texas.

Petkovic, G, et al., (1992). "Limit States for Concrete Cylinders and Beams," SINTEF Structures and Concrete, STF70 F92196, Trondheim, Norway.

PMB Systems Engineering Inc. (1984). *Seismic Analysis Procedures for Gravity Based Structures*, Vol. 1 and Vol. 2, Report to Den Norse Stats Oljeselskap A/S, Stavanger, Norway.

Scanlan, R. H. (1976). "Seismic Wave Effects of Soil-Structure Interaction," Earthquake Engineering and Structural Dynamics, John Wiley & Sons, London, UK.

Schneider, J. F., Stepp, J. C., and Abrahamson, N. (1992). "The Spatial Variation of Earthquake Ground Motion and Effects of Local Site Conditions," *Proceedings 10th World Conference on Earthquake Engineering*, Madrid Spain.

Sleefe, G. E. (1990). "The Long-Term Measurement of Strong-Motion Earthquakes offshore Southern California," Proceedings Offshore Technology Conference, OTC 2345, Society of Petroleum Engineers, Richardson, Texas.

Smith, C. E. (1997). "Dynamic Response of a Steel-Jacket Platform Subject to Measured Seafloor Earthquake Ground Motions," *Proceedings Eighth International Conference on the Behavior of Offshore Structures*, Vol. 3, Pergamon, Elsevier Science Ltd., Oxford, England.

Somerville, McLaren, Saikia, "Site Specific Estimation of Spatial Incoherence of Strong Ground Motion," *Earthquake Engineering and Soil Dynamics II - Recent Advances in Ground-Motion Evaluation*, Special Publication No. 20, American Society of Civil Engineers, New York.

Suharwardy, M. I. H., and Pecknold, D. A. (1978). *Inelastic Response of Reinforced Concrete Columns Subjected to Two-Dimensional Earthquake Motions*, Dept. of Civil Engineering, University of Illinois, Report UILU-ENG-78-2022, Urbana, Illinois.

Thompson, G. R., Foo, S. H. C., and Matlock, H. (1986). "Hibernia GBS Foundation Behavior," *Proceedings of the Third Canadian conference on Marine Geotechnical Engineering*, St. John's Newfoundland.

Veletsos, A. S. (1977). "Dynamics of Structure-Foundation Systems," *Structural and Geotechnical Mechanics*, W. J. Hall (Ed), Prentice-Hall, Inc., Englewood Cliffs, New Jersey.

Watson, P. G., and Randolph, M. F. (1997). "A Yield Envelope Design Approach for Caisson Foundations in Calcareous Sediments," Proceedings Eighth International Conference on the Behavior of Offshore Structures, Vol. 1, Pergamon, Elsevier Science Ltd., Oxford, UK.

Watt, B. J., (1978). "Dynamic Analysis of Concrete Gravity Structures," *Proceedings Deep-Sea Oil Production Structures*, University of California Extension Course, Berkeley, California.

Watt, B. J., Boaz, I. B., Ruhl, J. A., Dowrick, D. J., Shipley, S. A., and Ghose, A. (1978). "Earthquake Survivability of Concrete Platforms," *Proceedings Offshore Technology Conference*, OTC 3159, Society of Petroleum Engineers, Richardson, TX.

Whittaker, D. (1987). *Seismic Performance of Offshore Concrete Gravity Platforms*, Thesis, University of Canterbury, Christchurch, New Zealand.

Wolf, J. P. (1985). *Dynamic Soil-Structure Interaction*, Prentice-Hall, Inc., Englewood Cliffs, New Jersey.

Working Group on Quantification of Uncertainties (1986). *Uncertainty and Conservatism in the Seismic Analysis and Design of Nuclear Facilities,* Committee on Dynamic Analysis of the Committee on Nuclear Structures and Materials of the Structural Division of the American Society of Civil Engineers, New York.

Yokel, F. Y., and Bea, R. G. (1986). Mat Foundations for Offshore Structures in Arctic Regions, Report to Minerals Management Service, U. S. Dept. of Commerce, National Bureau of Standards, Gaithersburg, Maryland.

Young, A. G., et al. (1974). "Foundation Design of Offshore Gravity Structures," *Proceedings Offshore Technology Conference,* OTC 2371, Society of Petroleum Engineers, Richardson, Texas.

Zerva, A., and Harada, T. (1994). "A Site-Specific Model for the Spatial Incoherence of the Seismic Ground Motions," *Proceedings 5th U. S. National Conference on Earthquake Engineering,* Chicago, IL.

this page left blank intentionally

Appendix A

ISO Panel 5
Seismic Loading and Response
Draft Concrete Annex

October 1996

by V. Karthigeyan

INTRODUCTION

(Comments & topics for discussion by the panel and topics which is not clearly described are given in italics and in brackets. These are to be removed in the final draft)

NORMATIVE

CC 4 EARTHQUAKE DESIGN

This document provides the guidelines for strength and ductility requirements for seismic design of concrete platforms. These guidelines are based on the same principles as to those adopted for steel platforms in section C.4. Only the provisions that are different to steel platforms are given here and hence this document should be used in conjunction with C.4; in order to follow clauses and sections that are applicable to both steel and concrete platforms that are not repeated here. Some clauses such as C.4.2 are repeated with minor changes in full; in order to make it easier to follow.

The guidelines are applicable to all types of concrete platforms that are supported on the seafloor. They include Condeep/Seatank types as well as Manifold types.

This section does not cover techniques for modeling and analysis. See section 4/P11/WG4 for details.

CC 4.2 SEISMIC DESIGN PROCEDURE

Steps 1 through 12 in Fig. N1 and the list which follow define the integrated process that platform owners, their seismic consultants, and their design engineers must go through to develop criteria to design a concrete platforms which are supported on seabed.

Step 1 - Step 6 *(repeat from draft B2)*
Step 7 - Determination of biases and uncertainties for failure modes.
Step 8 - Evaluation of ductility requirements.
Step 9 - Determination of material coefficients or capacity reduction factors for failure modes.
Step 10 - Modeling for seismic analysis.
Step 11 - Response analysis.
Step 12 - Response assessment.

CC 4.2.2 Step 2: Evaluation of Seismic Activity by Zone

For concrete platforms the effective horizontal acceleration G shall be multiplied by a factor τ_h to account for the plan size of the platform.

(Table based on ref 6 to be evaluated?)
CC 4.2.4 Step 4: Shape of the Design Spectrum

(Modification of spectra to suit plan dimensions to allow for in coherence effect and wave passage effect ? Possible to achieve workable solution to met dead lines?)

Vertical spectrum shall be multiplied by a factor τ_v. τ_v should be assumed to be 1.0 unless a lower value is calculated based on depth of water and/or depth of foundation below seabed level.

CC 4.2.6 Step 6: SLE Load Factors

Values for the 200-year strength earthquake loading factor, γ_E, are summarized in the following table:

γ_E	seismotectonic zone			
	A	A/B	B	C
WG3 Level I	$1.6F_e$	$1.7F_e$	$1.9F_e$	$2.3F_e$
WG3 Level II				
WG3 Level III				

(0.4 was used for σ_{RE} . Values for Level I indicate that a separate table is hardly worthwhile - comments? Attempted to check values in Panel 5 draft. Level II & III answers did not correspond to my calculated values. To consult Bob Bea or Peter Marshall)

For conventional concrete platforms (Condeep or Seatank type) F_e may be assumed to be 0.75 where

$$F_e = [\mu\alpha]^{-1}$$

F_e may be reduced provided adequate lateral ties are provided to ensure large ductility ratios are possible (ref 4 & 9) or μ is evaluated from push over analysis. For manifold and other types of platforms μ and α should be evaluated from push over analysis.

(ref 9 indicates μ of over 4.5 can be achieved for concrete shaft provided adequate ties can be provided. Ref 1 indicate very low ductility 1.5 for Gullfaks A platform. More information is being sought from panel members and other sources to check whether a lower default value may be recommended for F_e)

CC 4.2.7 Step 7: Capacity Biases and Uncertainties

These are used to derive resistance factors for seismic loading (Step 9).

The bias is defined as the ratio of expected resistance in the failure made to that predicted by the code, they are also given for concrete, reinforcement ad pre-stressing as the ratio of actual mean values to nominal or characteristic values. *(May differ due to definition of characteristic values in different codes)*

CC.4.2.8 Step 8: Ductility Criteria

If the structure is of seatank or condeep type and located in zones of high storm intensity and low earthquake intensity and detailed adequately as to be ductile (ref 4 & 9), a ductility evaluation is not required and F_e may be assumed to be 0.75.

44

(Examples of push-over analysis are required to check whether less stringent requirements can be specified. Examples of push-over analysis with detailing in accordance with recommendations of refs are required to enable the requirement to be waived ?)

Ductility evaluation should always be carried out for manifold type platforms with the deck support frame forming a relatively soft story.

If static push-over analysis are used to evaluate the ductility characteristics of the platform, the following Reserve Strength Factors (RSF's) must be demonstrated:

RSF	seismotectonic zone			
	A	A/B	B	D
SSL 3	3.0	3.3	3.7	5.4
SSL 2	2.4	2.6	2.9	3.9
SSL 1	2.0	2.1	2.3	2.8

Reserve Strength Factor (RSF) is defined as the ratio of lateral capacity required form the pushover analysis to the factored SLE design load.

Optionally, in lieu of doing a ductility check, it is permissible to use DLE actions with SLE elastic design factors, independent of detailing.

CC.4.2.9 Step 9: Resistance Factors

The following table shows resistance factors ϕ_E for seismic load cases:

Failure mode	ϕ_E
bending	0.8
shear	0.4

(the factors were calculated from only one ref. Hence the following higher values are not presented: bending Normal density concrete - 0.84, LWA concrete - 0.89, shear with or without shear reinforcement - 0.44, shear with axial compression shear reinforcement - 0.6)

CC.4.2.10 Step 10: Structural Modeling

See section 4/WG4/P11 for detail guide to structural modeling.

CC.4.2.11 Step 11: Response Analysis

See section 4/WG4/P11 for detail guide to structural analysis.

CC.4.2.12 Step 12: Response Assessment

In calculating forces and moments in elements, the earthquake loading shall be combined with those due to gravity, hydrostatic pressure, and buoyancy.

All critical locations shall be strength checked for forces and moments caused by the action of these factored loads, and the following expression met:

$$\phi_E R_E \geq 1.1D_1 + 1.1D_2 + 1.1L_1 + \gamma_E E$$

Where D_1, D_2 and L_1 include only those parts of each mode of operation that might reasonably be present during an earthquake.

When internal forces due to gravity Loads or prestress opposes the inertial forces due to earthquake loads, the gravity and prestress load factors shall be reduced, and the following expression satisfied:

$$\phi_E R_E \geq 0.9D_1 + 0.9D_2 + 1.1L_1 + \gamma_E E$$

Where D_1, D_2 and L_1 are reduced to include only loads reasonably certain to be present.

(Knut Hove to comment on separating prestress load/displacement. VK to follow up the format of draft by P12/WG4)

INFORMATIVE ANNEX

INFO CC.4.1 GENERAL

These provisions were developed by Panel 5 of WG3 and is based on the work carried out by the same panel for steel platforms.

Scope

The ISO provisions were based on the work carried out by Bob Bea during the past 8 years for steel template/jacket type platforms. The formulations developed have been extended to cover concrete platforms.

Most of the concrete platforms installed so far have been in zone 1. Hence the experience in analyzing and designing for earthquake is limited and the knowledge gained is almost entirely from the design of nuclear installations which are smaller in size and can be usually located in good site conditions.

The above factors lead to some of the default values used in the normative being conservative. Reduction factors to account for the plan dimensions are likely to counterbalance this conservatism. It is hoped that the details contained in the informative will be used more extensively than for steel platforms and the experience gained will lead to the refinement of the formulations used.

Info CC.4.2.4 Step 4: Shape of Zone based SLE Spectrum, with system Ductility Effects

Unlike Jacket type steel platforms most concrete platforms are founded on sea bed. Hence the 50% reduction normally applied to steel platforms will not apply unless skirts are used to transfer vertical loads to lower stratum. Since water can carry compression waves, the augmentation of vertical waves at seabed level may not be fully realized. (*more guidance to be based on work by CB and Dolan*).

Elastic response spectra is presented for 5% damping. For concrete structures during the SSL earthquake the internal damping will be around 3%. Higher damping will be mobilized in soil due to radiation. These may be apparent in the first few modes at smaller frequencies in which mode shapes indicate foundation participation. Section 4/P11/WG4 contains more details of the damping values to be expected.

Info CC.4.2.4 Step 5: SLE Load Uncertainties

Tests indicate (ref 5) that ductilities of up to 4.5 can be achieved for concrete shafts by proper detailing. Since ductility characteristics of a concrete platform involve the displacement of foundation as well as rotation of the shaft, it is not possible to adopt high ductility values in calculating load factors γ_E. The results of push-over analysis (ref 1) indicate a ductility ratio μ of 1.5 and residual strength ratio α of nearly 0.9. Hence a default value of 0.75 is adopted for F_e in the following expression:

46

$$F_e = [\mu\alpha]^{-1} = 0.75$$

Unlike a jacket type structure with X braces, there is no redundancy in a concrete platform and most of the deflection is at foundation level or at the caisson/shaft junction. In addition at the top of caisson is a step change in stiffness. Hence the default value for F_e should not be reduced without a push-over analysis.

Info CC.4.2.6 Step 6: SLE Load Factors, γ_E

The three categories of uncertainties in tables 6 (σSE) & 7 (σGS) together with σRS are combined develop the resultant uncertainty in the earthquake induced forces, σE, as follows:

$$\sigma_E^2 = \sigma_{SE}^2 + \sigma_{GS}^2 + \sigma_{RS}^2$$

In comparison to 0.3 assumed by Bea a value of 0.4 has been assumed for σ_{RS} to account for larger uncertainties in hydrodynamic effects and added mass for concrete platforms.

The values for γ_E have been based on the following relationship:

$$\gamma_E = F_e \exp(0.8 \, \beta_E \, \sigma_E - 2.57 \, \sigma_E)$$

γ_E	σ_E							
SSL	0.8	1.0	1.2	1.4	1.6	1.8	2.0	2.2
1	0.42	0.36	0.31	0.27	0.23	0.20	0.17	0.15
2	0.65	0.63	0.61	0.59	0.57	0.55	0.53	0.51
3	1.02	1.11	1.20	1.30	1.40	1.51	1.64	1.77

Earthquake load factor γ_E based on loading uncertainties, σ_E and SSL's
for $F_e = 0.75$

Info.CC.4.2.7 Step : Element Capacity Biases and Uncertainties

The available bias and uncertainties for the materials and resistance given in refs 2 & 7 are summarized below:

	B_{RE}	σ_{RE}
Material		
Concrete compressive strength	1.1	0.10
tensile strength	1.2	0.15
Reinforcement, yield stress	1.12	0.06
Prestressing wire strength	1.06	0.04
Resistance of concrete 'beams'		
Bending		
- ND Concrete	1.13	0.10
- LWA Concrete	1.27	0.12
Shear		
- without shear reinforcement	1.48	0.41
- with shear reinforcement	1.23	0.35
- with axial compression		
no shear reinforcement	1.22	0.24

Info.C.4.2.8 Step 8: Ductility Criteria

Since the experience in overload performance of concrete platforms are limited and abrupt changes in stiffness in the vertical configuration of the platform σ_{PC} for the platform capacity is assumed to be 0.4.

The reserve strength factor RSF is calculated from bias and uncertainty using the following:

$$RSF = \exp\left[\beta_E(\sigma - 0.8\,\sigma_E)\right]$$

where $\sigma^2 = \sigma_E^2 + \sigma_{PC}^2$

These provide values which are slightly higher than those for jacket structures.

References

1) Booth E D & Roberts C J B - Response to Extreme Earthquakes of an Offshore Concrete Gravity Platform in the North Sea. Earthquake Engineering Britain, Thomas Telford Ltd, London 1985.

2) Det Norske Veritas Rules for Classification of Fixed Offshore Installations, Part 3 Chapter 1 Structural Design, General July 1995.

3) Fjeld Svein - Reliability of Offshore Structures Journal of Petroleum Technology Vol 29, 1.

4) Hove Knut - Ductility Design of Pre-stressed Tubular Shafts Subjected to Extreme Seismic Loading.

5) Kiureghian Armen Der (1992) - Response Spectrum Method for Multi-Support Seismic Excitations Earthquake Engineering and Structural Dynamics Vol 21 1992.

6) Kiureghian Armen Der (1996) - A coherency Model for Spatially Varying Ground Motions Earthquake Engineering and Structural Dynamics Vol 25.

7) Moan Torgeir - Safety Levels Across Different Types of Structural Forms and Materials - Implicit in Codes for Offshore Structures, SINTEF April 1995.

8) Norwegian Standard NS 3473 E Concrete Structures Design Rules Nov 1992.

9) Whittaker D - Seismic Performance of Offshore Concrete Gravity Platforms, Thesis, University of Christchurch New Zealand January 1988.

Background for Proposed
ISO Earthquake Guidelines
For Steel, Template-Type Platforms

PROBABILITY BASED LRFD PROCEDURE

The probability based earthquake LRFD procedure is outlined in Fig. 1. The procedure is based on the API LRFD formulation for design of the elements that comprise offshore platforms (API, 1993; Moses, 1986):

$$\phi_E \, R_E \geq \gamma_{D1} \, D_1 + \gamma_{D2} \, D_2 + \gamma_{L1} \, L_1 + \gamma_E \, E \dotfill (B.1)$$

where ϕ_E is the resistance factor for earthquake loadings, R_E is the design capacity of the platform element (e.g. brace, joint, pile) for earthquake loadings as defined by the API RP 2A - LRFD guidelines, γ_{D1} is the self-weight of the structure (dead) loading factor, D_1 is the design dead loading, γ_{D2} is the imposed equipment and other objects loading factor, D_2 is the design equipment loading, γ_{L1} is the consumables, supplies, and vessel fluids (live) loading factor, L_1 is the live loading, γ_E is the earthquake loading factor, and E is the earthquake loading effect developed in the structure or foundation element.

This development addresses the definition of the resistance factor, ϕ_E, and the loading factor, γ_E, for loadings induced by earthquakes. The dead, equipment and live loading factors will be taken as recommended in the API LRFD guidelines ($\gamma_{D1} = \gamma_{D2} = \gamma_{L1} = 1.1$) (API, 1993).

The probability based reliability background for this LRFD development is summarized in Appendix A.

This discussion will follow the numbered steps identified in Fig. B.1. As for development of the API LRFD guidelines, the earthquake loading effects and platform element capacity parameters will be based on a Lognormal format. Uncertainties will be expressed with the Standard
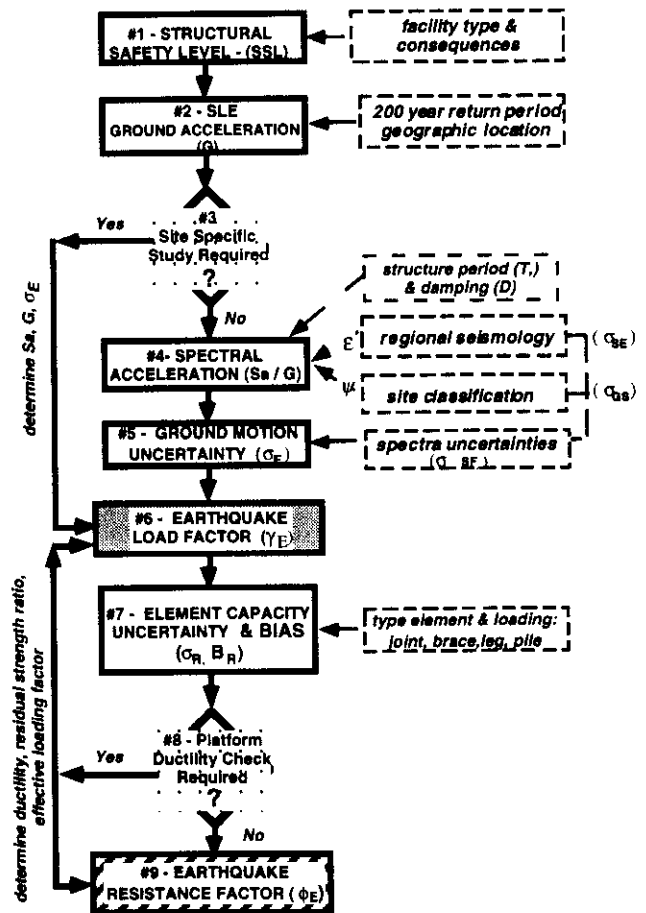

Fig. B.1 - Probability based LRFD procedure

Deviation of the Logarithms of the loading and capacity variables, σ.

STEP #1

The first step in the procedure is to define the Structural Safety Level (SSL) for the proposed platform. Four SSL's are identified.

SSL #1 would be associated with a platform that had low potential consequences associated with its loss of serviceability. Unmanned, shallow water (≤ 100 ft.) structures such as well protectors, freestanding / guyed / braced caissons, and tripods supporting minimum processing facilities, without significant oil storage, and equipped with shut-in devices to control hydrocarbon escape from wells and pipelines are examples of SSL #1 structures. Failure of such structures would not endanger surrounding facilities or life nor result in significant pollution consequences.

Table 1 - Structure Safety Levels, consequences, β_E's, and Pf's

SSL	Potential Consequences	β_E	Pf_{annual}	Pf_{life} annualized
#1	low	2.3	1E-2	9E-3 to 1E-2
#2	moderate	3.0	1E-3	1E-3 to 7E-4
#3	high	3.7	1E-4	1E-4 to 2E-5
#4	very high	--	--	--

SSL #2 would be associated with a platform that had moderate potential consequences associated with its loss of serviceability. Intermittently manned or manned-evacuated well protectors or minimum facilities production platforms with little oil storage, and fully equipped with shut-in devices to control hydrocarbon spillage from wells and pipelines are examples of SSL #2 structures. Failure of such structures would not endanger surrounding facilities or life nor result in more than moderate pollution consequences.

SSL #3 would be associated with a platform that had high potential consequences associated with its loss of serviceability. Unmanned, intermittently manned or manned-evacuated well protectors, or minimum facilities production platforms, with little oil storage, and fully equipped with shut-in devices to control hydrocarbon spillage from wells and pipelines are examples of SSL #3 structures. For such structures, provisions would be made so that personnel could be evacuated before (storms) or immediately after (earthquakes) a design event with reasonable certainty. Failure of such structures would likely result in potentially significant pollution consequences.

SSL #4 would be associated with a platform that had very high potential consequences associated with its loss of serviceability. Major, manned, drilling and or production platforms, supporting large to very large production equipment and significant oil storage, large permanent quarters, and located where evacuation of personnel before a design event is either not possible or is logistically very difficult are examples of SSL #4 structures. Failure of such a structure would result in potentially severe pollution consequences, endanger life, and have national / international implications.

Three SSL's have been identified with three annual target Safety Indices, β_E, for earthquake loadings (Bea, 1990; 1991; 1993; 1992). These Safety Indices are intended to apply to design of the platform elements controlled by earthquake loadings. The Safety Indices are summarized in Table 1 together with the annual and 'annualized' lifetime (20 years) probabilities of failure. The annualized (lifetime probability of failure divided by 20) lifetime probabilities of failure have been computed assuming perfect independence and dependence of the platform capacity from year to year. Due to their unique characteristics and importance, SSL #4 platforms would be addressed on a case-by-case basis utilizing an approach similar to that outlined here.

Appendix B details two complimentary approaches that can be used to determine the acceptable or desirable reliability associated with different types and categories of structures. The approaches include economic, historic performance, and standard-of-practice.

STEP #2

The next step in the process is to determine the Earthquake Hazard Zone (EHZ) for the platform based on its geographical location. The world's offshore areas have been divided into five EHZ's. These zones are associated with specified expected (mean) annual maximum SLE effective ground (rock) accelerations, G, that have average annual return periods of $T_{SLD} = 200$ years.

Examples of the EHZ are shown in Figs. B.2 through B.12. The EHZ's include Europe, North and South America, Central America, Africa, Middle East, East Asia, South Asia, the South Pacific, and the regions surrounding Japan and Indonesia. The EHZ have been based on results from recent site specific seismic exposure studies provided by members of the ISO Technical Committee (refer to Acknowledgments for names of committee members). Table 2 summarizes the EHZ and the associated 200 year return period SLE G's. The areas identified as 'A' through 'D' designate different types of seismotectonic zones. These designations will be discussed in Step #4.
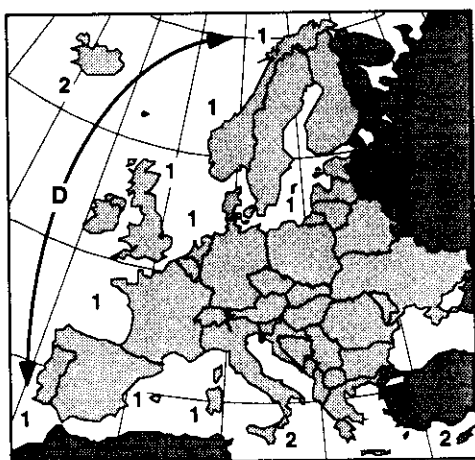
Fig. B.2 - Europe EHZ
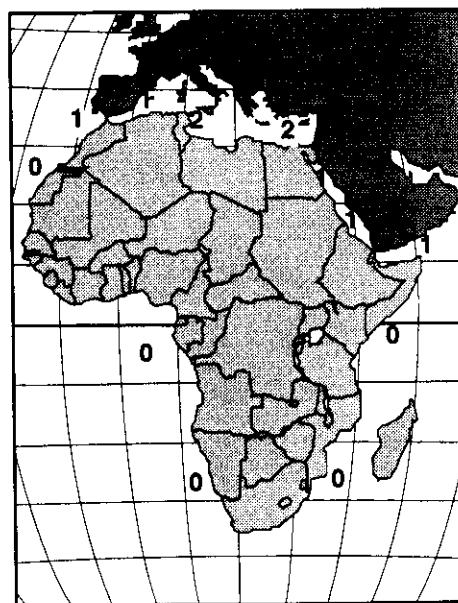

Fig. B.4 - South America EHZ
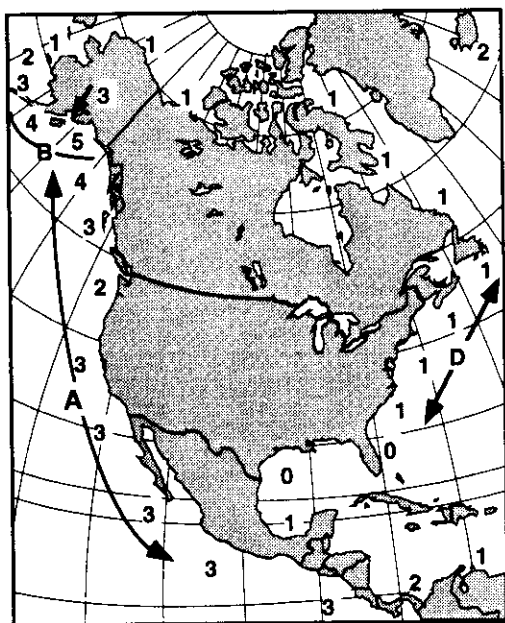
Fig. B.3 - North America EHZ

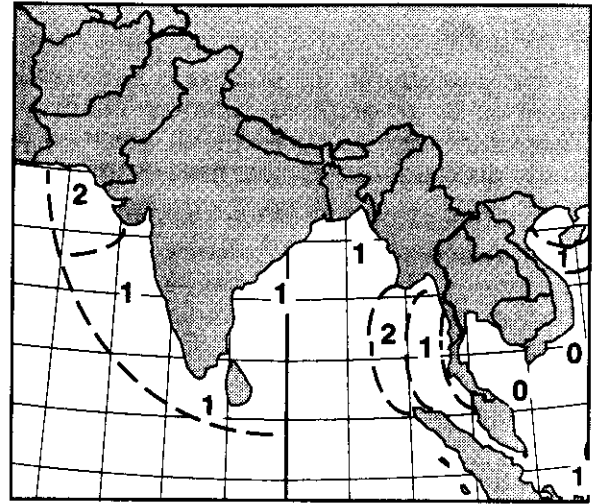**Fig. B.5 - Africa EHZ**
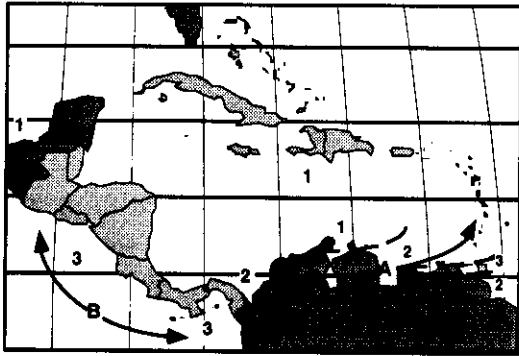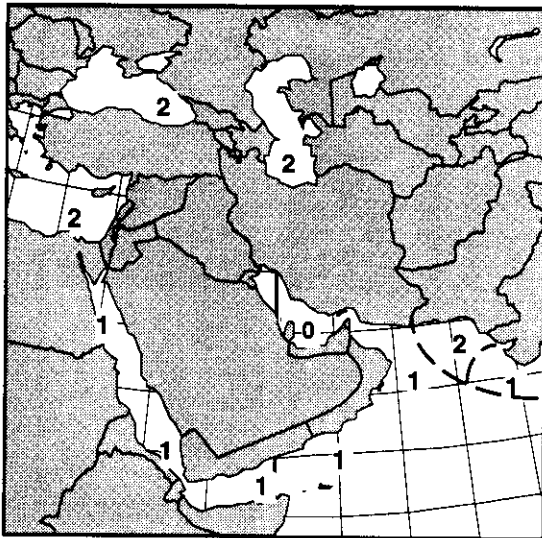
Fig. B.6 - Central America EHZ

Fig. B.7 - Middle East EHZ

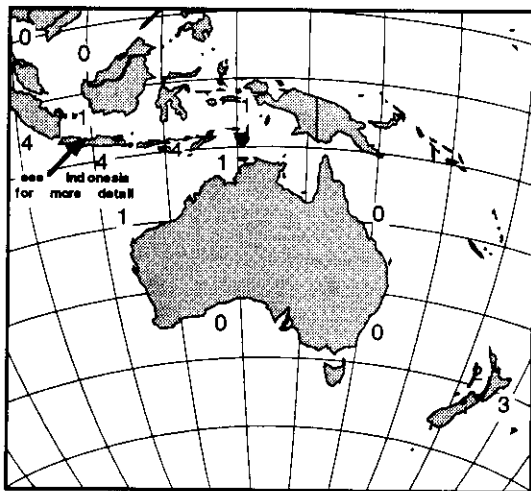Fig. B.8 - South Pacific EHZ

Fig. B.9 - South Asia EHZ
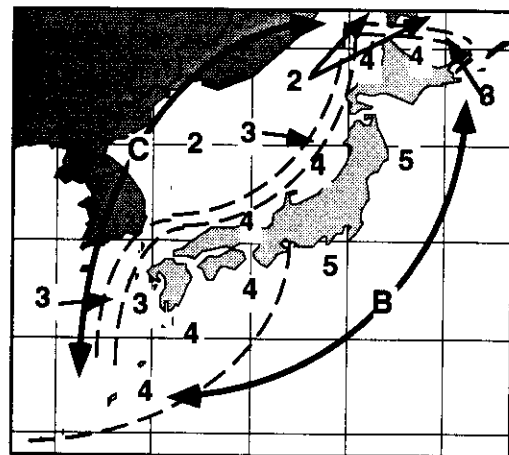

Fig. B.10 - East Asia EHZ
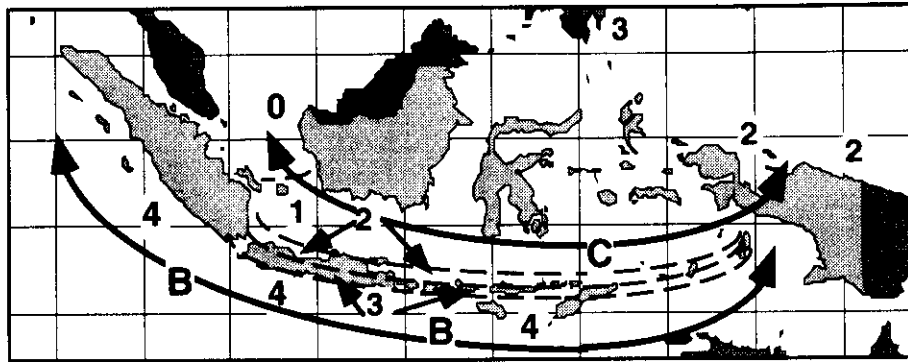

Fig. B.11 - Japan Region EHZ

52

Fig. 12 - Indonesia Region EHZ

STEP #3

In the third step, the engineer must determine whether or not a site specific seismic exposure study should or must be performed (Table 2). For SSL's ≥ 2 and EHZ ≥ 1, the platform owner and design engineer are encouraged to perform site specific seismic exposure studies that will characterize the parameters identified in this process including expected ground (rock) accelerations that have average annual return periods of T_{SLD} = 200 years (including attenuation uncertainties) and the elastic response spectra parameters that will be defined in subsequent steps.

For SSL #3, all EHZ of .3 or greater must determine G and other seismic exposure characteristics based on a site specific study. Site specific studies are encouraged for all EHZ for SSL #3 platforms. For SSL #2, all EHZ of 4 or greater must determine G and other seismic exposure characteristics based on a site specific study. All SSL #1 engineering can be based on these guidelines.

In some areas, site specific studies have been performed to determine the 100-year return period earthquake peak ground acceleration. To convert the 100-year G to the 200-year G, the following relationship can be used:

$$G_{200} = G_{100} \exp (0.24 \; \sigma_{SE}) \dotfill (B.2)$$

where σ_{SE} is the uncertainty in the long-term distribution of G (assumed to be Lognormally distributed). This parameter will be further discussed in Step #5.

STEP #4

The fourth step is to define the shape of the normalized mean (average) elastic principal horizontal acceleration response spectra (Fig. B.13) component. This shape is a function of the platform modal period, T, the local geology and soil conditions reflected in the parameter, y, and the regional seismotectonic characteristics reflected in the parameter, ε.

The response spectra is developed for a modal viscous damping ratio of D = 5 %. The mean or expected spectral accelerations, Sa, are identified in Fig. 13. When it can be justified, other values of the modal damping ratio, D (%),
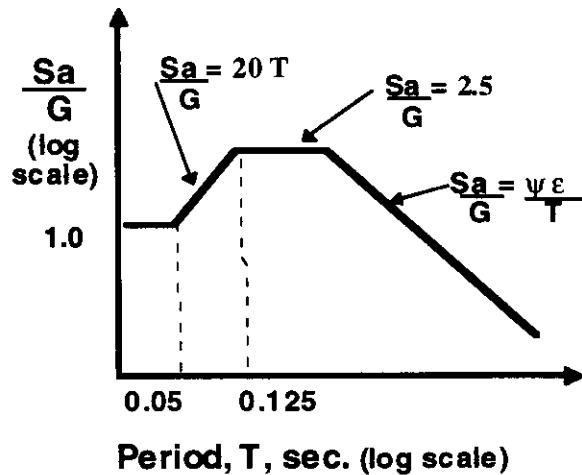

Fig. B. 13 - Elastic design response spectra

Table B.2 - Earthquake hazard zones, SLE ground accelerations and Structural Safety Levels

Zone	SLE G % g	SSL #1	SSL #2	SSL #3	SSL #4
0	0 - 5	Allowed			MUST
1	5 -15	to use		Should do site	DO
2	15 -25	these		specific study	SITE
3	25 -35	guidelines			SPECIFIC
4	35 -45				STUDY
5	45 -55				

can be used with the ordinates of the response spectra multiplied by the factor K:

$$K = 0.33 \, \text{Ln} \, (100 \, / \, D) \quad \text{...} \quad (B.3)$$

Table B.3 summarizes recommendations for the local geology and soil conditions parameter (ψ) and the seismotectonic characteristics parameter (e). The soil conditions are described in terms of five Site Classifications (SC - A through SC - E), alluvium thickness, H, and average shear wave velocities Vs (fps = feet per second) (Crouse, McGuire, 1994; Martin, Dobry, 1994; Borcherdt, 1994).

SC - E soil conditions are represented by profiles susceptible to failure or potentially liquefiable under seismic loading, and very thick (H > 200 feet) accumulations of soft to medium stiff clays. For Category E conditions, site and soil specific laboratory and analytical studies are required to characterize the site response characteristics and their influence on the elastic response spectra shape and ordinates.

The seismotectonic characteristics of the various offshore areas are described in terms of four classifications identified as types 'A' through 'D'. These classifications are identified on the EHZ maps in Figs. 2 through 12. The four classifications include shallow crustal faulting zones (e.g. offshore California and Venezuela, Type A), deep subduction zones (e.g. eastern Japan, Aleutian arc of Alaska, Type B), mixed shallow crustal and deep subduction zones (e.g. northern Indonesia, Cook Inlet, Alaska, Type C), and intraplate zones (e.g. North Sea, east coast of Canada, Type D). A default value of e = 1.0 can be used when the seismotectonic conditions are not defined.

The response spectra in the orthogonal horizontal direction should have the same characteristics as that in the principal direction. The ordinates of the response spectrum for the vertical direction should have values that are one-half of those of the principal horizontal response spectrum. For platforms supported by deeply embedded piles, the vertical spectra should be those representative of the soils along the lower portion of the piles (API, 1993).

Table B.3 - Local geology and soil conditions parameter, ψ, and seismotectonic characteristics parameter, ε

Soil Conditions		Seismotectonic Conditions	
Site Classification	ψ		ε
SC - A Rock (Vs ≥ 2,500 fps)	1.0	Type A Shallow crustal faulting zones	1.0
SC - B Stiff to very stiff soils, gravels (Vs = 1200 to 2500 fps)	1.2	Type B Deep subduction zones	0.8
SC - C Sands, silts, and very stiff clays (Vs = 600 to 1200 fps)	1.4	Type C Mixed shallow crustal & deep subduction zones	0.9
SC - D Soft to medium stiff clays (H = 10 to 200 ft.; Vs ≤ 600 fps)	2.0	Type D Intraplate zones	0.8
		Default value	1.0
SC - E **Site specific studies required**			

For intense earthquake motions that force the platform system into nonlinear, inelastic response, the ductility and residual strength characteristics of the platform have important effects on the ordinates of the elastic response spectra (Miranda, Bertero, 1994; Bea, Young, 1993; Bazzurro, Cornell, 1994; Cornell, 1995). In the development of the loading factors, the effects of the ductility have been integrated into the effective earthquake loading factor, Fe.

The platform system ductility, μ, is defined as the ratio of the maximum lateral displacement, Δp, (e.g. measured at the deck elevation) that can be developed without collapse of the platform (unable to support gravity loadings) to the displacement at which the first significant nonlinear behavior is apparent in the response of the system, Δe (μ = Δp / Δe). The platform residual strength ratio, α, can be characterized as the ratio of the area under the platform load- to ultimate displacement diagram, A, divided by the area under an ideal elasto-plastic load to ultimate displacement diagram that has the same peak lateral load resistance, Aep (α = A / Aep).

For conventional template-type, drilling and production platforms, based on results from current evaluations of the ductility characteristics of well designed platforms in which the platform element capacities were defined according to API RP 2A - LRFD guidelines (Bea, et al, 1987; Bea, Young, 1993; Bazzurro, Cornell, 1994; Bea, Landeis, Craig, 1992; Hellan, Tandberg, Hellevigt, 1992) the mean ductility is presumed in this development as μ ≥ 2.5 and the mean residual strength ratio as a ≥ 0.8. The mean earthquake effective loading factor, Fe, is taken to be the reciprocal of the product of these two quantities (Bea, 1992; Bea, Young, 1993; Miranda, Bertero, 1994):

$$Fe = [\, \mu\, \alpha\,]^{-1} = 0.5 \dotfill (B.4)$$

Present API guidelines specify vertical diagonal bracing patterns for primary load carrying trusses that are acceptable in the jackets of template-type platforms. Vertical bracing patterns for SSL's and representative values of μ and α for these bracing patterns (joints and compactness meet API guidelines and moderately loaded decks) are summarized in Table B.4 (Bea, 1992; Bea, Young, 1993; Bea, Landeis, Craig, 1992; Brazzurro, Cornell, 1994; Hellan, Tandberg, Hellevigt, 1992; Smith, 1994; Dolan, Crouse, Quilter, 1992).

STEP #5

Table B.4 - Vertical truss bracing patterns suggested for SSL's and associated μ and α

| SSL	Vertical Truss Bracing Pattern	μ	α
#1	Vertical or horizontal K	1.5	0.7
#2	Vertical K with full horizontal framing	2.0	0.8
#3	X -braced or X-braced combined with Vertical K with horizontal framing	2.5	0.8

This step is concerned with evaluation of the uncertainties associated with the elastic response spectra ordinates and the methods used to determine the forces induced in the platform elements by earthquakes.

Each of the geographic regions (Fig. B.2 - B.12) has associated with it an inherent variability due to the seismic sources and source-to-site attenuation characteristics. In this development, it is assumed that this variability is defined by the standard deviations of the logarithms of the annual expected effective horizontal ground accelerations on rock, G, having average return periods in the range of 200 years to several thousand years (Fig. B.14). This parameter is identified as σ_{SE}. This parameter represents the inherent variability associated with the seismotectonic environment (seismic sources, seismicity) and the transmission of earthquake energy from the seismic sources to the local site (attenuation relationships).

The uncertainty in the peak ground acceleration can be determined from the following relationship:

$$\sigma_{SE} = 0.39 \, (\ln G_{10} - \ln G_1) \dots \dots \dots (5)$$

where G10 and G1 are the 10-year, and 1-year return period expected peak ground accelerations, respectively.
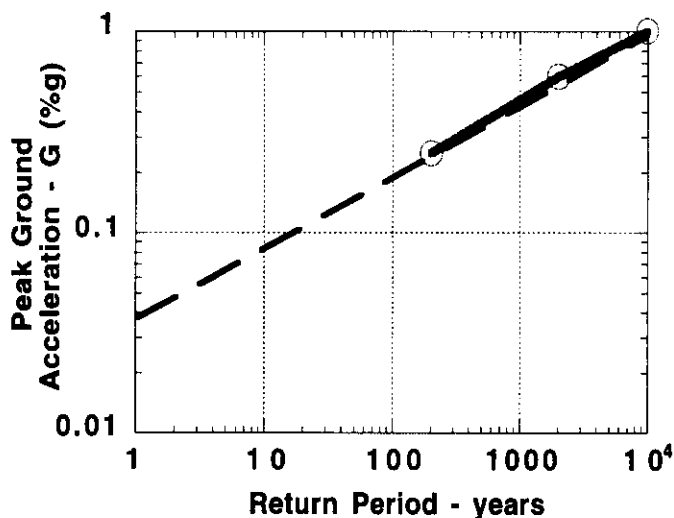
Fig. B.14 - Determination of uncertainty in ground accelerations

Table B.5 - Seismic sources & earthquake attenuation uncertainties

Location	σ_{SE}
California	1.0
Gulf of Alaska / Aleutian Region	1.3
Alaska (St George, Bristol Bay)	1.1
Cook Inlet	1.2
E. Coast Canada (Newfoundland)	1.7
North Sea	2.0
Venezuela (Cristobal Colon)	0.8
New Zealand (Maui)	1.3
Japan (E. Coast)	1.4
Caspian Sea (Azeri)	1.0
Sakhalin Island	0.8
Australia (NW Shelf)	1.7
Indonesia (N. coast)	1.3
Mediterranean (Sicily)	0.9

Based on presently available results from seismic exposure studies provided by the ISO Panel 5 members, site specific values for σ_{SE} are given in Table B.5. Based on this information, generalized values for σ_{SE} as a function of the seismotectonic characteristics of the region in which the site is located are summarized in Table B.6.

As indicated in Fig. B.1, the next category of uncertainty, σ_{GS} is related to the local geology and soil conditions and their effects on the ordinates of the response spectra. Based on results from recent studies of the effects of local geology and soil conditions on elastic response spectra, Table 7 summarizes preliminary recommendations for this category of uncertainty (Crouse, McGuire, 1994; Miranda, Bertero, 1994).

The third category of uncertainty relates to the response spectrum method used to determine forces in the elements that comprise the platform. This uncertainty includes the modeling uncertainties contributed by evaluation of the platform mode shapes, periods, and masses (including hydrodynamic effects, $\sigma \approx 0.15$); the combination of modes ($\sigma \approx 0.15$); and damping (structural, hydrodynamic, foundation, $\sigma \approx 0.15$), and the uncertainties associated with "ductility" reductions in the elastic response spectra ordinates ($\sigma \approx 0.15$). An uncertainty of $\sigma_{RS} = 0.30$ has been used as the base case value (Bea, 1991; Bea, Landeis, Craig, 1992).

The three categories of uncertainty are combined to develop the resultant uncertainty in the earthquake induced forces, σ_E, as follows:

$$\sigma_E{}^2 = \sigma_{SE}{}^2 + \sigma_{GS}{}^2 + \sigma_{RS}{}^2 \dots\dots\dots\dots\dots\dots\dots\dots\dots\dots\dots\dots (B.6)$$

Table B.6 - Seismic sources and attenuation uncertainties

Seismotectonic Characteristics	σ_{SE}
Type A Shallow crustal fault zones	1.0
Type B Deep subduction zones	1.4
Type C Mixed shallow crustal fault and deep subduction zones	1.2
Type D Intraplate zones	2.0

STEP #6

With the results developed in the preceding five steps, the engineer is ready to determine the earthquake loading factor, γ_E. Values for γ_E are summarized in Fig. B.15 for the three SSL's, Fe = 0.5, and a representative range in σ_E. The values for have been based on the following relationship (Bea, 1992):

$$\gamma_E = Fe \exp (0.8 \beta_E \sigma_E - 2.57 \sigma_E) \dots\dots\dots\dots\dots\dots (B.7)$$

When explicit ductility analyses are required (Step #8) and Fe ≠ 0.5, the values in Fig. 15 should be multiplied by 2 Fe for the Fe determined from the ductility analyses.

Table B.7 - Uncertainties associated with local geology and soil conditions

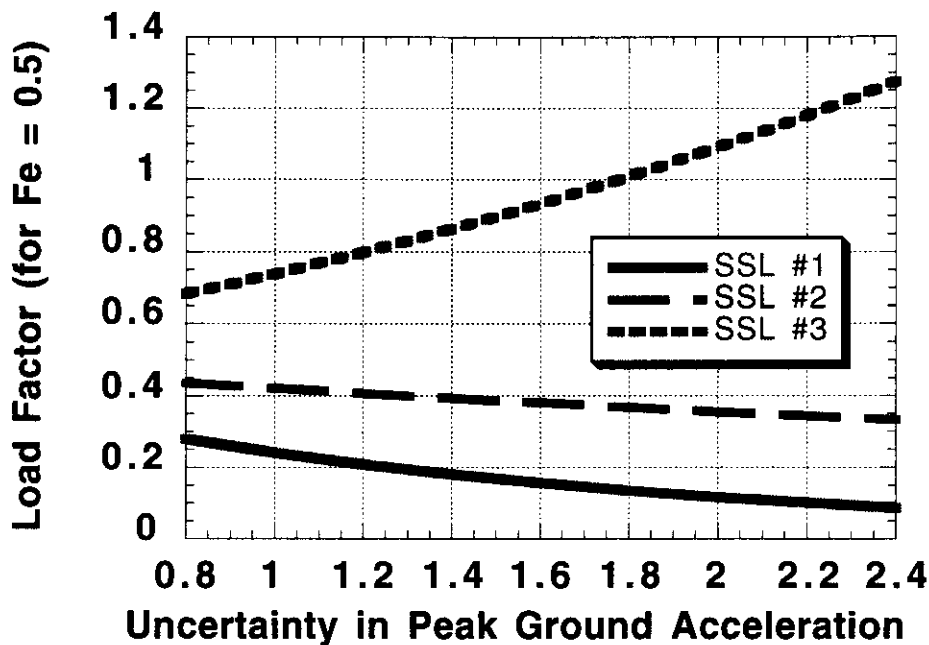| Geology / Soil Conditions	σ_{GS}
SC - A	0.30
SC - B	0.40
SC - C	0.40
SC - D	0.50
SC - E	0.50

Fig. B.15 - Load factors for earthquake loadings

As would be expected, the earthquake loading factor is smaller for lower consequence SSL's. Somewhat paradoxical for SSL #1 and #2 is the reduction in the earthquake loading factor for greater seismic loading uncertainties. For SSL #3 the earthquake loading factor increases as the uncertainty in the earthquake loadings increases. Fig. B.16 illustrates the reason for this paradox. It is a consequence of adopting the expected 200-year return period earthquake loading for all SSL's. To eliminate this paradox one would need to develop seismic exposure maps for appropriate design return periods for each of the SSL's, making the design return periods smaller for the lower consequence SSL's.
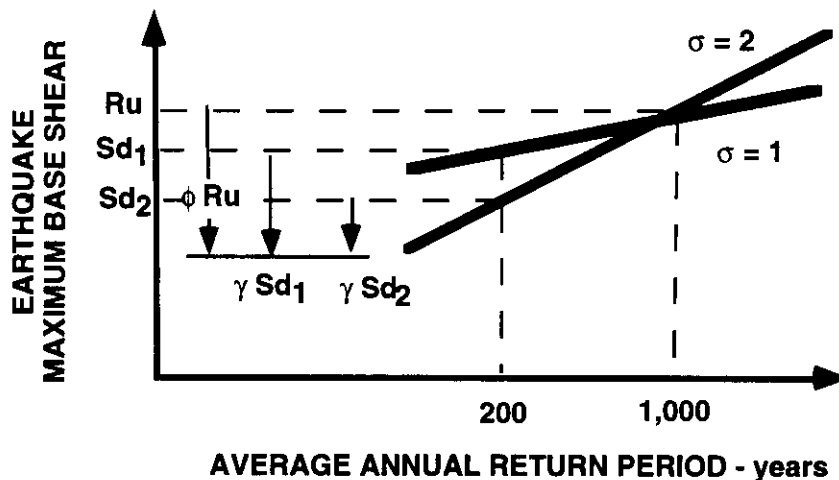

Fig. B.16 - Reduced load factors for larger seismic loading uncertainties

STEP #7

The next step in the process is to evaluate the 'biases' and uncertainties involved in the evaluation of the platform element static loading (design) capacities, R_E. The design capacities that are referenced are those specified in API RP 2A - LRFD. The term bias is defined as the ratio of the true or expected capacity of the element subjected to earthquake loading effects to the predicted or design code nominal value of the capacity (generally, the static capacity).

The mean or expected biases, B_{RE}, and uncertainties, σ_R, of the platform structure element capacities have been evaluated by Moses (1986), Ekngesvik, et al. (1987), and by Tang (1988, 1990) for the platform foundation elements. Based on this background, example mean biases and uncertainties for the structure and foundation elements are summarized in Table 8. In final form, this table would contain additional details on all structural and foundation elements and the various modes of loading.

The biases shown in Table B.8 for the foundation elements are dependent on details of how the soils are sampled, tested, and analyzed and the imposed loadings. Table B.9 summarizes the evaluation of bias in the axial pile capacity of a pile driven into normally consolidated clays. The reference characteristics for a bias of unity are shown together with other conditions and the associated bias for the given condition.

Table B.8 - Structure & foundation capacity biases and uncertainties

Elements	Uncertainties	
	B_{RE}	σ_{RE}
T, Y, DT Joints		
-compression	1.5	0.15
-tension	2.0	0.40
K Joints		
-axial	1.6	0.20
-in plane bending	1.8	0.15
-out of plane bending	1.6	0.15
Tubular Braces		
- tension	1.3	0.10
- comp.	1.4	0.15
- bending	1.5	0.10
- hydrostatic	1.4	0.10
Piles axial loads		
- clays	2.5	0.40
- sands	1.0	0.50
lateral loads		
- clays	1.5	0.30
- sands	1.1	0.40

Table 9 - Bias in axial pile capacity in normally consolidated clays

Component	Reference	Condition and Mean Bias
Boring	Drill mud	Sea water **1.2**
Sampling	Push sampling	Wireline **1.5 - 2.0**
Testing	Remolded reconsolidated direct simple shear	Unconfined compression **1.5 - 2.0**
Characterization	Upper bound of data	Lower bound **1.5 - 2.0**
Loading	Static	Storm - **2.0** Quake - **2.5**
Analysis	T-Z degrading	Limit equilibrium **1.2 - 1.3**
Age	10 years	10 days **1.5**

59

STEP #8

If the platform is a conventional template-type drilling and production platform that meets the API RP 2A - LRFD configuration (e.g. bracing arrangements and member compactness requirements) and sizing guidelines, a ductility evaluation is not required. For conventional platforms, this development has been based on $\mu \geq 2.5$, $\alpha \geq 0.8$.

For non-conventional platforms, or when the platform designer deems that is it prudent, a platform system ductility evaluation should be performed as outlined in the API RP 2A guidelines and the ductility, residual strength ratio, and effective loading factor determined (Eq. B.7).

If time history ductility analyses are used, the guidelines suggest using three or more representative ground motion time histories based on results from a site specific hazards study.

Average return periods, T_{DLE}, for the ground motions for the three SSL DLE ground motions are summarized in Table B.10. These return periods have been based on the following (Bea, 1992).

Table B.10
DLE time history return periods

SSL	Average Return Period (years)
#1	---
#2	$\approx 1,000$
#3	$\approx 10,000$

$$T_{DLE} = 2.1 \exp(\beta_E \delta)^{1.6} \quad\quad\quad\quad\quad\quad (B.8)$$

where δ is the uncertainty ratio (ratio of the total uncertainties in the seismic loading effects and platform loading capacity to the uncertainties in the seismic loading effects). No DLE requirements are identified for SSL #1. For the seismic conditions considered in this development, δ is in the range of 1.01 to 1.07.

If static push-over analyses are used to evaluate the ductility characteristics of the platform, the dynamic / transient loading nonlinear response effects incorporated into Fe must be recognized in definition of the required Reserve Strength Ratio. This will require performing push-over analyses that are displacement controlled after the first major nonlinear events occur in the structure system. Such analyses are able to accurately define the ductility and residual strength ratio.

Table B.11 summarizes the required RSR's as functions of the SSL's and the uncertainty in the seismic loading environment, σ_E. An uncertainty in the platform capacity of $\sigma_{PC} = 0.30$ has been assumed (Bea, 1992; Ekngesvik, Olufsen, Karuanakaran, 1987). The RSR's in Table 11 have been based on the following with Fe = 0.5 (Bea, 1992):

$$RSR = Fe \exp(\beta \sigma - 2.57 \sigma_E) \quad\quad (B.9)$$

where σ is the resultant uncertainty in the seismic loading effects and the platform seismic loading capacity:

Table B.11 - Static reserve strength ratios, RSR, for Fe = 0.5 referenced to 200-year unfactored design loading

(multiply by 2Fe for other Fe's)

SSL	$\sigma_E = 0.8$	$\sigma_E = 1.0$	$\sigma_E = 1.5$	$\sigma_E = 2.0$
#1	--	--	--	--
#2	0.8	0.9	1.0	1.3
#3	1.5	1.8	3.0	5.2

$$\sigma^2 = \sigma_E^2 + \sigma_{PC}^2 \quad\quad\quad\quad\quad\quad\quad\quad\quad\quad (B.10)$$

An alternative definition of the platform over-load capacity is the Reserve Strength Factor (RSF). The RSF is the ultimate lateral load capacity of the platform divided by the factored design loading:
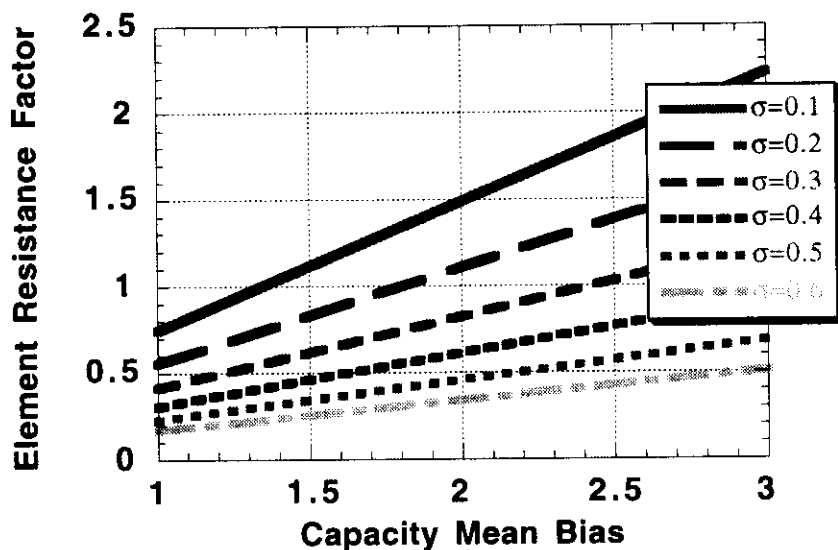
$$RSF = \exp [\beta (\sigma - 0.8 \sigma_E)] \dots\dots\dots\dots\dots\dots\dots\dots\dots\dots\dots\dots\dots\dots\dots\dots\dots\dots\dots\dots(B.11)$$

STEP #9

The last step is to determine the platform element resistance factor, ϕ_E. The resistance factors are evaluated based on the following expression:

$$\phi_E = B_{RE} \exp (-0.8 \beta_E \sigma_{RE}) \dots\dots\dots\dots\dots\dots\dots\dots\dots\dots\dots\dots\dots\dots\dots\dots\dots\dots\dots(B.12)$$

The resistance factors for SSL #3 elements are summarized in Fig. B.17 as a function of the mean bias and uncertainty for the elements.

Fig. B.17 - Structure and foundation resistance factors for SSL #3

CONCLUSIONS

A probability based methodology has been used to develop earthquake load and resistance factors that have general and global applicability. This approach is proposed as a basis for the ISO guidelines for seismic loading and response of offshore platforms. It also could be used in a similar manner for other extreme environmental loading conditions.

Preliminary quantification of parameters in the approach have been provided to illustrate how it could be applied in development of earthquake load and resistance factors for the ISO guidelines. The approach and proposed quantifications have been verified with site specific results from four locations. Good agreements have been developed between the site specific results and those based on these guidelines.

The approach provides an important element of "information sensitivity" that allows the loading and resistance factors to be varied as a function of the desired SSL for a platform, the unique aspects of its seismic environment, and the primary uncertainties in the earthquake loadings and platform element capacities.

Key ISO Panel 5 future efforts will be directed at definition of the SSL's and their associated annual Safety Indices (Table 1), additional definition of the seismic exposure maps and references to the earthquake design guidelines of the associated countries, characterization of the seismic exposure, attenuation, and local geologic (soil response) uncertainties (Tables 5 - 7), detailing of the platform

element seismic capacity biases and uncertainties (Table 9), and additional site and platform specific verifications.

ACKNOWLEDGMENTS

REFERENCES

American Petroleum Institute, API (1993). Recommended Practice for Planning, Designing and Constructing Fixed Offshore Platforms. API Recommended Practice 2A (RP 2A) - LRFD. Twentieth Edition, August, Dallas, Texas.

American Petroleum Institute, API (1994). Proposed Revisions to RP 2A - WSD Recommended Practice for Planning, Designing, and Constructing Fixed Offshore Platforms - Assessment of Existing Platforms - Draft Section 17, November, Dallas, Texas

Bazzurro, P., and Cornell, C. A. (1994). "Seismic Hazard Analysis for Non-Linear Structures I: Methodology, and II: Applications," J. of Structures, American Society of Civil Engineers, New York, NY, Nov.

Bea, R. G. (1977). Oceanographic and Earthquake Criteria, The Gulf of Alaska Criteria and Platform Study. Report to American Petroleum Institute, Dallas, Texas, Nov.

Bea, R. G. (1979). "Earthquake and Wave Design Criteria for Offshore Platforms." J. of Structural Eng., American Society of Civil Engineers, Vol. 105, No. ST2, Feb.

Bea, R. G. (1990a), Reliability Based Design Criteria for Coastal and Ocean Structures. National Committee on Coastal and Ocean Engineering, The Institution of Engineers, Australia, Barton, ACT.

Bea, R. G. (1990b). "Reliability Criteria for New and Existing Platforms," Proceedings of the Offshore Technology Conference, OTC 6312, Houston, Texas, May.

Bea, R. G. (1991a). "Offshore Platform Reliability Acceptance Criteria," J. of Drilling Engineering, Society of Petroleum Engineers, June, pp. 131-137.

Bea, R. G. (1991b). Loading and Load Effects Uncertainties. Report to Canadian Standards Association, Verification Program for CSA Code for the Design, Construction and Installation of Fixed Offshore Structures Project No. D-3, October.

Bea, R. G. (1992). "Seismic Design and Requalification Methodologies for Offshore Platforms," Proceedings of the International Workshop on Seismic Design and Requalification of Offshore Structures, California Institute of Technology, Pasadena, CA, Dec.

Bea, R. G. (1993). "Reliability Based Requalification Criteria for Offshore Platforms," Proceedings of the 12th International Conference on Offshore Mechanics and Arctic Engineering, OMAE'93, Glasgow, Scotland, June.

Bea, R. G., and Young, C. N. (1993). "Loading and Capacity Effects on Platform Performance in Extreme Storm Waves and Earthquakes," Proceedings of Offshore Technology Conference, OTC 7140, Houston, Texas, May.

Bea, R. G., Audibert, J. M. E., and Akky, M. R. (1979). "Earthquake Response of Offshore Platforms." J. of Structural Eng., American Society of Civil Engineers, Vol. 105, No. ST2, Feb.

Bea, R. G., Landeis, B., and Craig, M. J. K (1992). "Re-qualification of a Platform in Cook Inlet, Alaska," Proceedings Offshore Technology Conference, OTC 6935, Houston, Texas, May.

Bea, R. G., Mosaddad, B., Vaish, A. K., and Ortiz, K. (1987). Seismic Load Effects Study. Report to the American Petroleum Institute, Dallas, Texas, Nov.

Borcherdt, R. D. (1994). "Estimates of Site-Dependent Response Spectra for Design (Methodology and Justification)," Earthquake Spectra, The Professional Journal of the Earthquake Engineering Research Institute, Vol. 10, No. 4, Nov.

Cornell, C. A. (1994). "Risk-Based Structural Design," Proceedings of a Symposium on Risk Analysis, University of Michigan, Ann Arbor, Michigan.

Crouse, C. B. And McGuire, J. W. (1994). "Site Response Studies for Purpose of Revising NEHRP Seismic Provisions," Proceedings SMIP 94 Seminar on Seismological and Engineering Implications of Recent Strong-Motion Data, California Division of Mines and Geology, Sacramento, CA.

Dolan, D. K., Crouse, C. B., and Quilter, J. M. (1992). "Seismic Reassessment of Maui A." Proceedings Offshore Technology Conference, OTC 6934, May.

Ekngesvik, K., Olufsen, A., and Karunakaran, D. (1987). Literature Survey on Parameter Uncertainties Related to Structural Analysis of Marine Structures, SINTEF Report, N-7034, Trondheim-NTH, Norway.

Hellan, Ø., Tandberg, T., and Hellevigt, N. C. (1992). "Nonlinear Re-Assessment of Jacket Structures Under Extreme Storm Cyclic Loading," Proceedings of the Offshore Mechanics and Arctic Engineering Conference, OMAE'93, Glasgow, Scotland, June.

Martin, G. R. and Dobry, R. (1994). "Earthquake Site Response and Seismic Code Provisions," National Center for Earthquake Engineering Research (NCEER) Bulletin, Vol. 8, No. 4, Oct.

Miranda, E. and Bertero, V. V. (1994). "Evaluation of Strength Reduction Factors for Earthquake-Resistant Design," Earthquake Spectra, Vol. 10, No. 2, Berkeley, California.

Moses, F. (1986). Development of Preliminary Load and Resistance Design Document for Fixed Offshore Platforms. Final Report to the American Petroleum Institute, Dallas, Texas, Jan.

Smith, C. E. (1994). "Dynamic Response of Offshore Steel-Jacket Platforms Subject to Measured Seafloor Seismic Ground Motions," Ph. D. Dissertation, George Washington University, March.

Tang, W. H. (1988). Offshore Axial Pile Design Reliability. Report to the American Petroleum Institute, March.

Tang, W. H. (1990). Offshore Lateral Pile Design Reliability. Report to the American Petroleum Institute, Aug.

van de Graaf, J. W., Tromans, P. S., and Efthymiou, M. (1994). "The Reliability of Offshore Structures and Its Dependence on Design Code and Environment," Proceedings of the Offshore Technology Conference, OTC 7382, Houston, Texas, May.